IVYSPRING INTERNATIONAL PUBLISHER

Theranostics

2019; 9(11): 3223-3248. doi: 10.7150/thno.31844

Review

AIE-based theranostic systems for detection and killing of pathogens

Xuewen He[1,3#], Ling-Hong Xiong[2#], Zheng Zhao[1,3], Zaiyu Wang[1,3], Liang Luo[4], Jacky Wing Yip Lam[1,3], Ryan Tsz Kin Kwok[1,3]✉, Ben Zhong Tang[1,3,5]✉

1. Department of Chemistry, Hong Kong Branch of Chinese National Engineering Research Centre for Tissue Restoration and Reconstruction, Institute for Advanced Study and Division of Life Science, The Hong Kong University of Science and Technology, Hong Kong
2. Shenzhen Center for Disease Control and Prevention, Shenzhen 518055, China
3. HKUST-Shenzhen Research Institute, Shenzhen 518057, China
4. National Engineering Research Center for Nanomedicine, College of Life Science and Technology, Huazhong University of Science and Technology, Wuhan 430074, China
5. NSFC Center for Luminescence from Molecular Aggregates, SCUT-HKUST Joint Research Laboratory, State Key Laboratory of Luminescent Materials and Devices, South China University of Technology, Guangzhou 510640, China

#These authors contribute equally.

✉ Corresponding author: E-mail: chryan@ust.hk and tangbenz@ust.hk

© Ivyspring International Publisher. This is an open access article distributed under the terms of the Creative Commons Attribution (CC BY-NC) license (https://creativecommons.org/licenses/by-nc/4.0/). See http://ivyspring.com/terms for full terms and conditions.

Received: 2018.11.28; Accepted: 2019.03.05; Published: 2019.05.18

Abstract

Pathogenic bacteria, fungi and viruses pose serious threats to the human health under appropriate conditions. There are many rapid and sensitive approaches have been developed for identification and quantification of specific pathogens, but many challenges still exist. Culture/colony counting and polymerase chain reaction are the classical methods used for pathogen detection, but their operations are time-consuming and laborious. On the other hand, the emergence and rapid spread of multidrug-resistant pathogens is another global threat. It is thus of utmost urgency to develop new therapeutic agents or strategies. Luminogens with aggregation-induced emission (AIEgens) and their derived supramolecular systems with unique optical properties have been developed as fluorescent probes for turn-on sensing of pathogens with high sensitivity and specificity. In addition, AIE-based supramolecular nanostructures exhibit excellent photodynamic inactivation (PDI) activity in aggregate, offering great potential for not only light-up diagnosis of pathogen, but also image-guided PDI therapy for pathogenic infection.

Introduction

Pathogen definition and traditional detection and killing methods

Pathogens are infectious microorganisms or agents that can cause diseases[1]. They include bacterium, virus, protozoa, prion and fungus[2]. Bacteria are typically ranging between 1 and 5 μm in length. By varying in the cell wall structure and chemical components, bacteria can be simply divided into Gram-positive (G^+) and Gram-negative (G^-) subtypes. The infections caused by bacteria are the most prominent underlying reasons of many severe diseases, such as pneumonia, sepsis, septic arthritis, dermatosis and inflammatory bowel disease, which have increasingly raised medical and public concerns across the world[3]. For example, up to 50,000 deaths in the USA are linked with *S. aureus* infections each year[4]. Viruses typically range between 20 and 300 nm in length. Diseases like smallpox, influenza, mumps, measles, chickenpox and Ebola are caused by the viral infection[5]. Fungi with typical spore size of 1 ~ 40 μm in length, comprising a eukaryotic kingdom of microbes that are usually scavengers and consume dead organisms, can also cause diseases in humans,

animals and plants[6].

The sensitive detection and identification of pathogens are the fundamentally important tasks for human health. Several techniques are available, including plating and culturing, immunological approaches (enzyme-linked immunosorbent assay, ELISA), nucleic acid probe-based methods (polymerase chain reaction, PCR). Some new strategies for pathogen detection, such as microarrays analysis, microfluidic based analytical devices, electrochemical sensors, and flow cytometric methods etc, have been developed in recent year.[7-11]. However, the utility of these methods is generally limited by instrumental dependence, time-consuming and complexity in operation[12]. Effective killing of pathogens is another important goal to achieve. Bacterial infection can often be treated by using antibiotics, which could destroy the bacterial membrane, target its peptidoglycan, and effect the bacterial metabolism process and DNA, RNA, or protein synthesis. Once the bacterial DNA is expelled, it is incapable of protein synthesis and then dies[13]. While viruses are generally treated with antiviral compounds[14]. Unfortunately, with the abuse of antibiotics for identification and treatment of pathogens during the last few decades, multidrug resistant (MDR) pathogenic infection has become one of the most serious threats in the world[15]. In addition, due to the special biostructure and robust propagation ability, treatment of eukaryotic fungal pathogens requires extra efforts for specific drugs designing, as they may be more resistant to antibiotics[16].

AIE principle, advantage, and application in pathogenic detection and killing

Fluorescence imaging with advantages of easy operation, rapidness, excellent sensitivity, and specificity, is essential for in situ visualization of bioanalytes at the molecular level and monitoring complicated biological processes in real time[17, 18]. However, conventional fluorophores, such as fluorescein, rhodamine, BODIPY and cyanine, mostly emit brightly in dilute solution and undergo serious photobleaching and self-quenching at high concentration or in the aggregated state[19]. Although inorganic nanoparticles such as quantum dots or upconversion nanoparticles possess excellent brightness and photostability, their heavy metal components always cause toxicity concerns[20-32]. It is thus highly desirable to develop new fluorescent sensors with suitable biocompatibility and photostability that can efficiently conquer these shortcomings.

Unlike conventional organic fluorophores, luminogens with aggregation-induced emission (AIEgens) with propeller-shaped structures emerged as promising alternatives for turn-on fluorescent sensing [33]. As isolated molecules, the rotor-like AIEgens undergo low-frequency motions and dissipate exciton energy, leading to fast nonradiative decay and weak emission. Whereas, in the aggregated form, the radiative pathway dominates with strong emission via the restriction of intramolecular motion (RIM)[34]. Since the initiation of the concept of AIE in 2001[35], numerous AIEgens have been developed based on the RIM mechanism, such as silole[35], tetraphenylethene (TPE)[36], triphenylethylene (TriPE)[37], triphenylamine (TPA)[38], tetraphenyl imidazole (TPIM)[39], diphenyl isoquinolinium (IQ)[40], tetraphenylpyrazine (TPP)[41], pyrene[42] and other moieties-based derivatives (**Figure 1**, top). AIE aggregates exhibit large Stokes' shift, robust luminosity, strong photobleaching resistance, no random blinking and excellent biocompatibility. Accompanying with the foundation of varying aggregating mechanisms (**Figure 1**, below)[43], they have been widely applied for *in vitro* and *in vivo* biosensing and imaging[44-58]. Among them, various systems are synergistically integrated into specific and sensitive detection and differentiation of various pathogens[59].

Meanwhile, in the killing of pathogens, AIE-based supramolecular nanostructures with photodynamic inactivation (PDI) effect have become promising options for antimicrobial practices[60-62]. In general, photodynamic therapy (PDT) employs photosensitizers to absorb light and generate single excited state. The singlet excited state further transfers the energy to triplet excited state, which would sensitize the ambient triplet oxygen, resulting in the formation of destructive singlet oxygen or other reactive oxygen species (ROS)[63]. The ROS can oxidize bacterial cell membrane and intracellular DNA, RNA and lipids and subsequently lead to bacterial destruction. As it is unnecessary for photosensitizers to enter their cells, bacteria are relatively hard to develop resistance to PDI. However, the constant probe fluorescence of traditional photosensitizers makes it difficult to conduct real-time detection of bacteria without multiple washing steps. In addition, as most of them are hydrophobic, their binding interaction with bacteria could inevitably lead to aggregates formation, which will cause fluorescence quenching with reduced ROS generation[64]. Taking their unique advantages, AIEgens and their nanosized supramolecular structures can generate efficient ROS in the aggregated state. Thus, they could offer a great potential for not only light-up diagnosis of pathogens,

but also image-guided PDI therapy of pathogenic infection.

In this review, the powerful AIE-based theranostic systems for detecting and killing pathogens will be discussed in the following aspects, including: (I) amphiphilic AIEgens that self-assemble to form highly emissive supramolecular aggregates targeting pathogens through various noncovalent interactions, including electrostatic, hydrogen bonds, van der Waals, and metal-ligand interactions; (II) reactive AIEgens that are modified with recognition moieties and covalently linked with target molecules from pathogens to realize turn-on fluorescence; (III) reaction with enzymes or specific biospecies to cleave targeting groups on the AIEgens with structure changing or solubility decrease to light-up fluorescence; (IV) conjugation of AIEgens with functional ligands, such as peptides, polymers, nanoparticles and host-guest structures to target pathogens with turn-on fluorescence and enhanced antimicrobial outcomes; (V)self-assembly of AIEgens into nanoparticles or supramolecular nanostructures with intrinsic drug- or photo-activity for straightforward pathogenic theranostics; (VI) integration with existed analytic methods, such as fluorescent array (F-array) and ELISA for improved performance in sensitivity and specificity as well as convenience in signal read-out.

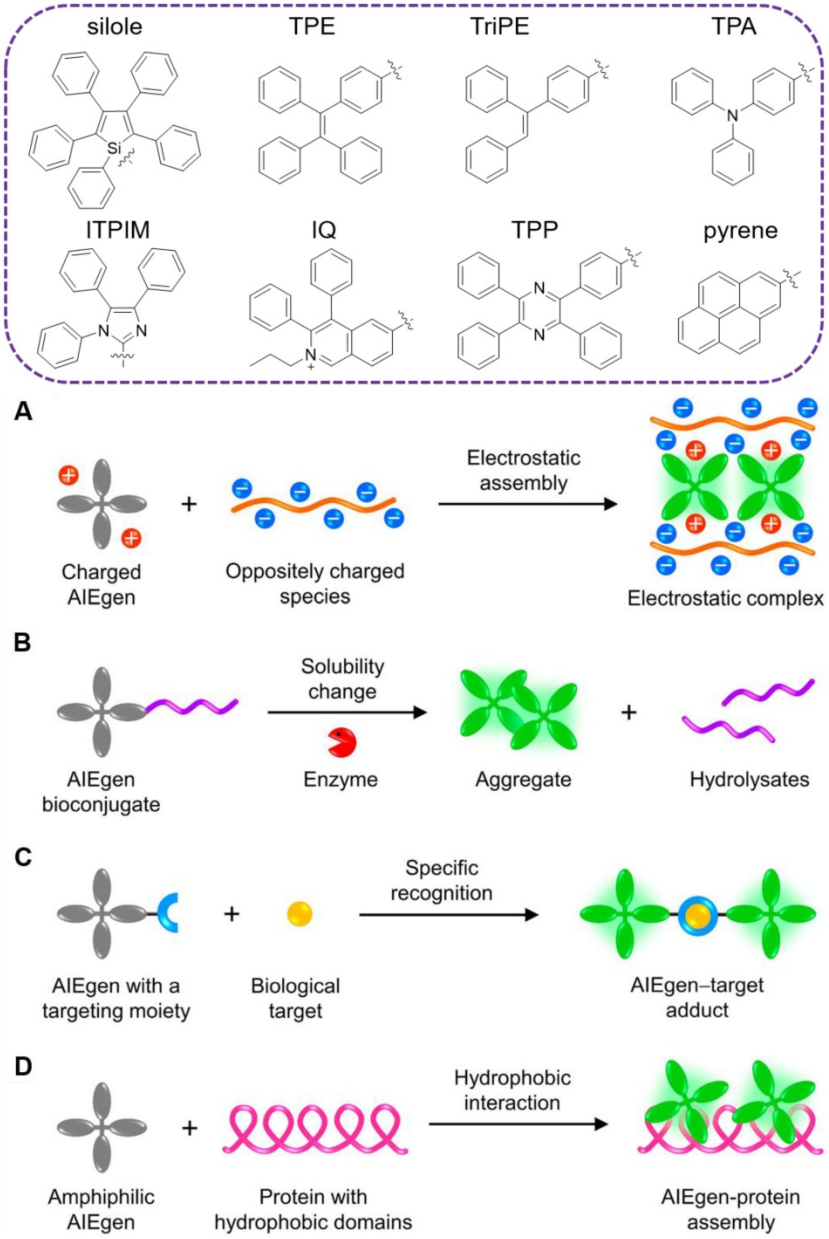

Figure 1. TOP: traditional moieties for construction of AIEgens. Below: schematic illustration showing the common working principles of AIE-based "turn-on" systems: **(A)** electrostatic assembly, **(B)** solubility change, **(C)** specific recognition and **(D)** hydrophobic interaction. Reproduced with permission from[43], copyright 2018 American Chemical Society.

Bacterial detection and killing

AIEgen derived systems

AIEgen-based amphiphilic molecules for bacterial imaging and killing

During the past decades, considerable efforts have been made to develop supramolecular assemblies by utilizing noncovalent interactions, such as electrostatic, hydrophobic, van der Waals and hydrogen bonding, and to investigate their applications in biosensing and imaging. Among the supramolecular assemblies, ionic self-assembly to couple different building blocks by electrostatic interactions possesses unique advantage in signal output between the molecular isolated and aggregated states. The formed supramolecular structures from amphiphilic molecules with AIE activity have been widely applied in bacterial sensing, imaging and killing.

In order to figure out the role of electrical charge in the interaction of AIEgens with various bacteria, Zhou's group designed a series of amphiphilic AIEgens with different positive, negative, or zero charges (**Figure 2**, top)[65]. They are constructed with TPE core and tailored with one or two quaternary ammonium, aldehyde or carboxylic acid groups. These TPE derivatives exhibited typical AIE features, superior resistance to photobleaching, and excellent bioimaging activity toward both G^+ and G^- bacteria. As the TPE substituted by quaternary ammonium (TPEMN and TPEDN) displayed much stronger emission after interaction with both G^+ and G^- bacteria comparing with the neutral TPEMA and TPEDA, the most significant role between AIEgens and bacteria was assigned to the electrostatic interaction. And hydrophobic interaction was inferior in their complexation with bacteria, as the negatively charged AIEgens behaved similarly as the neutrally charged counterparts. Moreover, the varying charged AIEgens were used as efficient artificial tongues for bacterial discrimination, in which eight kinds of bacteria, including three G^+ bacteria and five G^- bacteria were identified with 100% accuracy.

Similar to these dominated roles from electrostatic interaction, Tang's group also reported three types of positively charged AIEgens with different emission colors, namely IQ-naphthalene (Naph), IQ-diphenylamine (DPA), and IQ-triphenylamine (TPA), respectively (**Figure 2**, below)[66]. Due to their shared positive charge, all of these AIEgens could instantly image the *E. coli* in 10 min with robust fluorescence signal. Both live and dead bacteria can be stained by these AIEgens. Wash-step was not required during the staining and imaging, greatly simplifying the procedure and decreasing the imaging background. In addition, no dark-toxicity or phototoxicity was observed from these AIEgens towards the G^- bacteria.

In order to avoid the interference from the autofluorescence of microorganisms, Zeng's group rationally designed a charged tetraphenyl imidazole derivative AIEgen (TPIM-ClO_4) with far-red emission wavelength for bacterial imaging[39]. The TPIM-ClO_4 exhibited large Stokes shifts (225 nm), long emission wavelength (650 nm), excellent water solubility and photostability. The electron withdrawing unit of indolium was specifically incorporated to induce an intramolecular charge transfer (ICT) transition and thus make redshift of wavelength. Additionally, imidazolium had been widely applied as a suitable coordination site for anions via both electrostatic and hydrogen bonding interactions. As a result, anionic target, G^+ bacteria could be instantly imaged by TPIM-ClO_4 without washing process. Due to the abundance of negatively charged teichoic acids and thick peptidoglycan layers on their wall, G^+ bacteria could be specifically discriminated out from the bacterial mixture.

Apart from the typical AIE channeled fluorescence, Tang's group reported an excited-state intramolecular proton transfer (ESIPT) combined probe, 2-(2-hydroxyphenyl) benzothiazole (HBT-C18) for wash-free imaging of bacteria[67]. The HBT-C18 contained an intramolecular six-membered hydrogen bond and a C-N bond between the benzothiazole moiety and the substituted phenyl ring. Due to the ESIPT process, it exhibited "enol" and "keto" emissions, associated with normal and extremely large Stokes shift, respectively. The ratio of keto/enol emission was highly dependent on environmental polarity, as polar solvents can easily disrupt the intramolecular hydrogen bond. Based on the restriction of intramolecular rotation around the C-N bond and protection of the intramolecular hydrogen bond by close packing in the aggregated state, HBT-C18 exhibited typical AIE activity. By harnessing the negatively charged outer membrane of bacteria, it could image the G^- bacteria without any washing process.

Urinary tract infections mainly caused by uropathogenic *E. coli.* are severely afflicting human beings. As a characteristic component of the outer membrane of *E. coli.*, lipopolysaccharide (LPS) functions as an important biomarker for the detection of urinary tract infections[68]. For sensitive and specific detection of LPS in urinary tract infection, Wang and Li's group designed and synthesized an AIE probe (TPEPyE), bearing a positively charged pyridinium pendant[69]. Due to the phosphorylated

glucosamine sugars and the two 2-keto-3-deoxyoctonate units, bacterial LPSs are highly negatively charged substances, and could efficiently couple with the positively charged TPEPyE. Consequently, robust AIE fluorescence was triggered. The limit of detection (LOD) for LPS in artificial urine could be down to 4 nM. Moreover, due to the prevalence of LPS on the membrane of G$^-$ bacteria, TPEPyE could specifically differentiate them from G$^+$ bacteria.

With the urgent demanding of high throughput antibiotics screening and bacterial susceptibility evaluation, Tang's group developed a fluorescent method based on an amphiphilic AIEgen with positively charged amines and a long alkyl chain [70]. At concentrations below critical micelle concentration (CMC), the AIEgen emitted weakly. While in the presence of bacteria, its orange AIE fluorescence was turned on because of the binding driven by electrostatic force. As expected, the amphiphilic AIEgen could instantly stain both G$^+$ and G$^-$ bacteria without washing process. A wide detection range was achieved from 5 × 10^6 to 2 × 10^8 CFU/mL (colony-forming units per mL) with a LOD of 5.5 × 10^5 CFU/mL. Moreover, high throughput antibiotics screening and bacterial susceptibility evaluation could be finished in 5 h using this fluorescent assay, which was much shorter than traditional agar dilution or disk diffusion method.

The bacterial translocation is a serious issue, which results in severe liver disease, cancer and even death. Dynamic tracing and visualization of the bacterial translocation are always challenging topics in the illustration of therapeutic mechanisms. As stable fluorescent signals are necessitated in long-term monitoring, Tang's group developed a DPAS-based AIEgen containing morpholine and naphthyl units, namely 2-(((diphenylmethylene)hydrazono)methyl) naphthalene (M1-DPAN) with excellent photostability, for visualizing the infection processes of G$^+$ bacteria (**Figure 3**)[71]. To HeLa cells, *S. aureus* first got close and attached to the cells within 1 h, and invading processed within another 2 h. After 8 h, most of them crossed over the cancer cell membrane and wildly spread inside HeLa cells. The effect of antimicrobial agents, such as ethanol or bactericides, on the infection activity of bacteria could also be monitored in real-time. Faster than that of HeLa cells, *S. aureus* crossed the NIH 3T3 cell membrane in 3 h, and the apoptosis happened within 5 h.

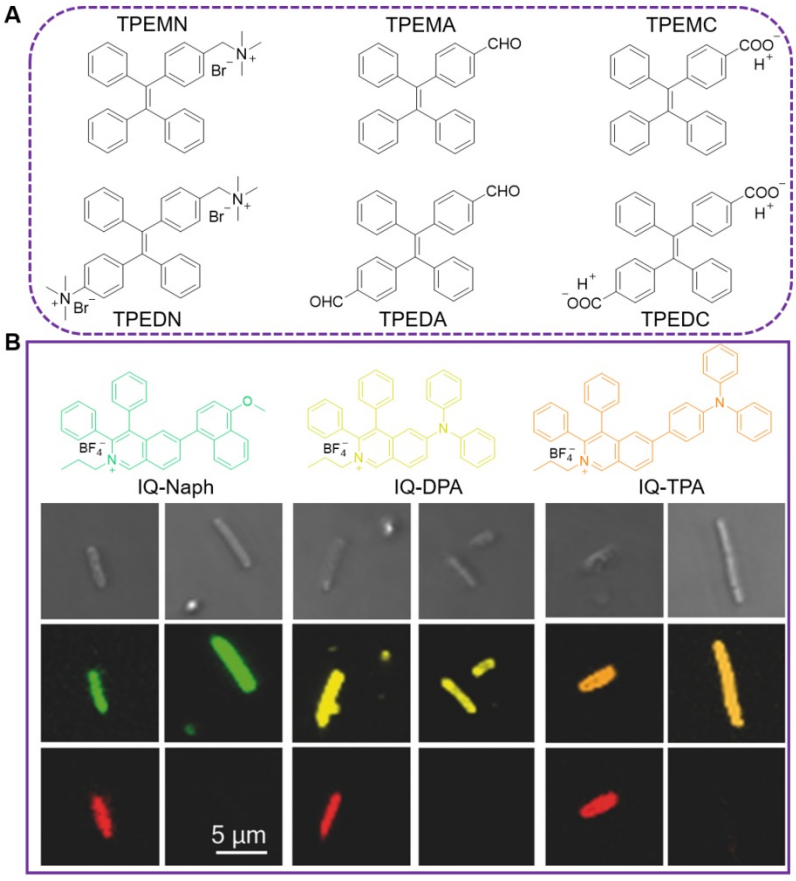

Figure 2. (A) AIEgens modified with momo- or dimer- charged group, named as TPEMN, TPEDN, TPEMA, TPEDA, TPEMC and TPEDC, respectively. **(B)** Molecular structures of IQ-Naph, IQ-DPA, and IQ-TPA and their application in bacterial imaging. Bright fields (row 1) and confocal images (row 2) of *E. coli* stained by IQ-Naph, IQ-DPA, or IQ-TPA, respectively, and co-stained with PI (row 3, red color). Reproduced with permission from [66], copyright 2018 Wiley-VCH.

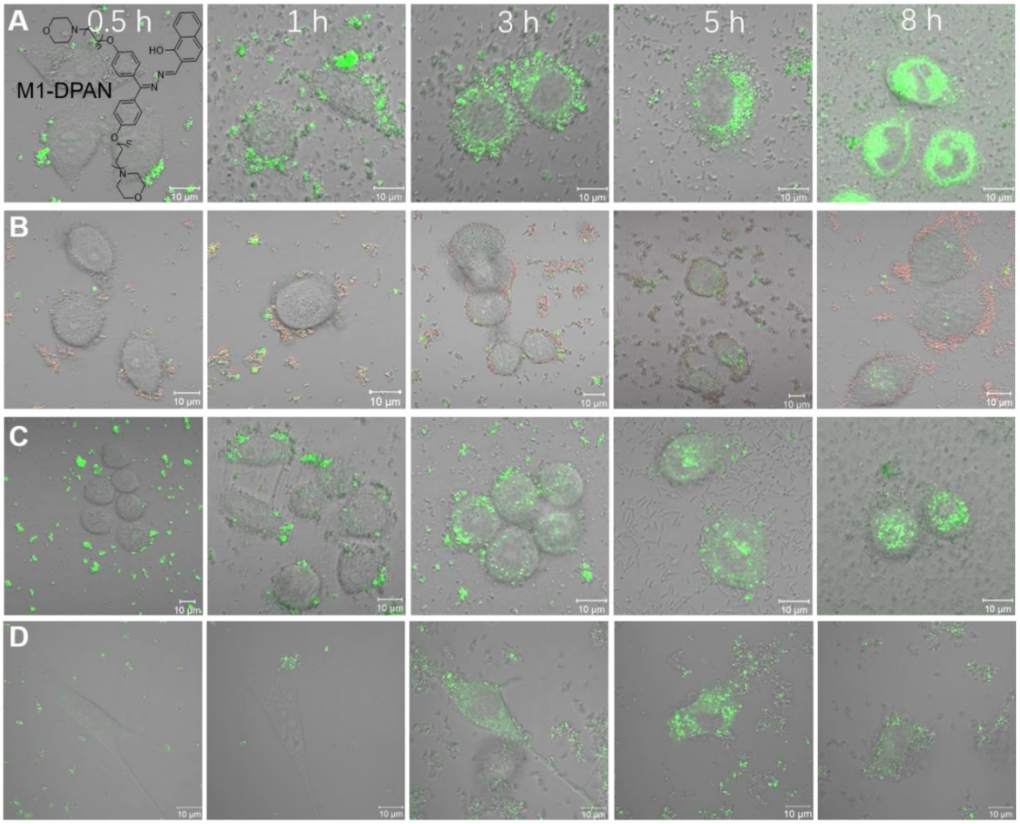

Figure 3. The CLSM images of HeLa cells infected by M1-DPAN-labelled **(A)** living *S. aureus*, **(B)** *S. aureus* treated by 75% EtOH and **(C)** *S. aureus* treated with cephalothin and PI. **(D)** The CLSM images of NIH 3T3 cells infected by M1-DPAN-labelled living *S. aureus*. Reproduced with permission from [71], copyright 2018 Elsevier.

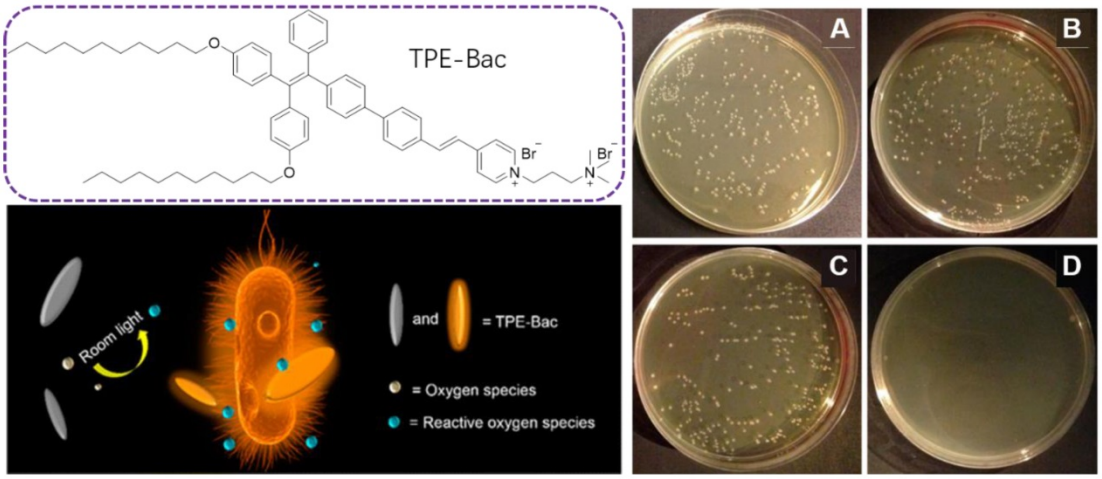

Figure 4. Molecular structure of TPE-Bac and schematic illustration of the ROS generation under room light for antibacterial practices. Plates of *E. coli* **(A)** without and **(B)** with light irradiation in the absence of TPE-Bac. **(C)** Pattern after storage in the dark or **(D)** Irradiation with room light. Reproduced with permission from [73], copyright 2015 American Chemical Society.

With the successful applications of light-induced ROS from AIEgens in killing cancer cells, PDI therapy has become a promising alternative for antibacterial activities. PDI is based on photosensitizers, which are nontoxic in the dark but are able to generate toxic ROS under light irradiation, leading to bacterial destruction. As ROS does not have a specific attacking target, it is very hard for bacteria to generate resistance for PDI, which should serve as a promising alternative for antibiotics[72]. Tang's group extended this PDI therapy into the bacterial imaging and elimination via a photo-active AIEgen, TPE-Bac(**Figure 4**) [73]. TPE-Bac could stain both G^+ and G^- bacteria in 10 min. No washing step was

required during the imaging of bacteria. The amphiphilic TPE-Bac bearing two long alkyl chains and two positively charged amines could intercalate into the membrane of bacteria, increase membrane permeability and lead to dark toxicity. TPE-Bac showed good photostability and could serve as a photosensitizer to induce ROS generation, which greatly enhanced the efficiency in killing of bacteria. The viability of G^+ and G^- bacteria treated with TPE-Bac and 10 min irradiation under room light, were 40% and 45%, respectively, both of which dropped to below 10% after another 20 min irradiation, and further decreased to less than 1% when the irradiation time up to 1 h.

Zhang's group further investigated the significant role of counter anion to the ROS performance of positively charged AIEgen, based on a pyridinium-substituted with an alkyne group (TPE-A-Py$^+$)[74]. TPE-A-Py$^+$ exhibited higher photosensitizing efficiency than TPE-Py$^+$ (lack of alkyne group) when I^- was used as a counter anion, as the calculated ΔE_{ST} between the excited singlet state and triplet state was much lower for TPE-A-Py$^+$ than for TPE-Py$^+$. Comparing to PF_6^-, $N(SO_2CF_3)_2^-$ and BPh_4^-, I^- countered PE-A-Py$^+$-entailing an alkyne bond displayed the highest photosensitizing performance. Moreover, as an outstanding photosensitizer, TPE-A-Py$^+$ could be used as PDI agent to kill both the G^+ and G^-bacteria, as well as the photo-inactivate ampicillin-resistant *E. coli*, under white-light irradiation within a few minutes.

Increasing studies showed that cancer-associated bacteria could increase the risk of distant metastasis and seriously reduce the cancer therapeutic efficiency[75]. Some bacteria in the tumor microenvironment were capable of enhancing chemo-resistance through metabolizing chemotherapeutic drugs and modulating the autophagy of cancer cells[76]. Thus, exploration of new approaches that enable selective differentiation and effective killing of both cancer cells and bacteria is of great value in the battle against cancers. Tang's group reported a versatile AIEgen (TPPCN) modified with positive charge (**Figure 5**)[77]. TPPCN showed intense AIE emission and efficient ROS production. It could selectively discriminate G^+ from G^- bacteria within 10 min, with the merits of superb sensitivity, good photostability, and a high signal-to-noise ratio. Additionally, TPPCN aggregates could efficiently generate ROS and selectively cause damage to G^+ bacteria under white light irradiation, with the cell walls shrunk and split as well as dramatical change in the shape. What's more, in a multi-component system containing cancer/normal mammalian cells and bacteria, the TPPCN could simultaneously differentiate and kill both cancer cells and G^+ bacteria.

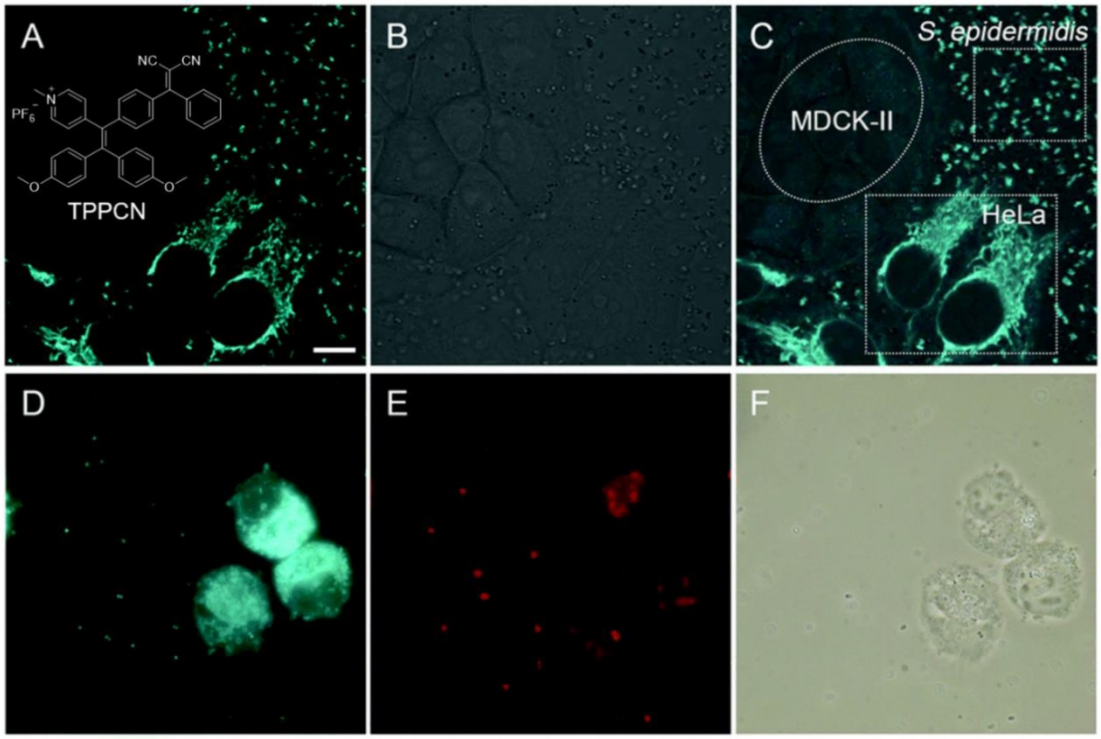

Figure 5. (A-C) Selective imaging of *S. epidermidis* and HeLa cells. **(A)** Fluorescence, **(B)** bright-field and **(C)** merged images of a mixture of S. epidermidis, HeLa and MDCK-II cells incubated with TPPCN. **(D-F)** Effective killing of S. epidermidis and HeLa cells. **(D)** Fluorescence images of a mixture of *S. epidermidis* and HeLa cells incubated with TPPCN. **(E)** After white light exposure. **(F)** Respective bright-field images. Reproduced with permission from [77], copyright 2018 Royal Society of Chemistry.

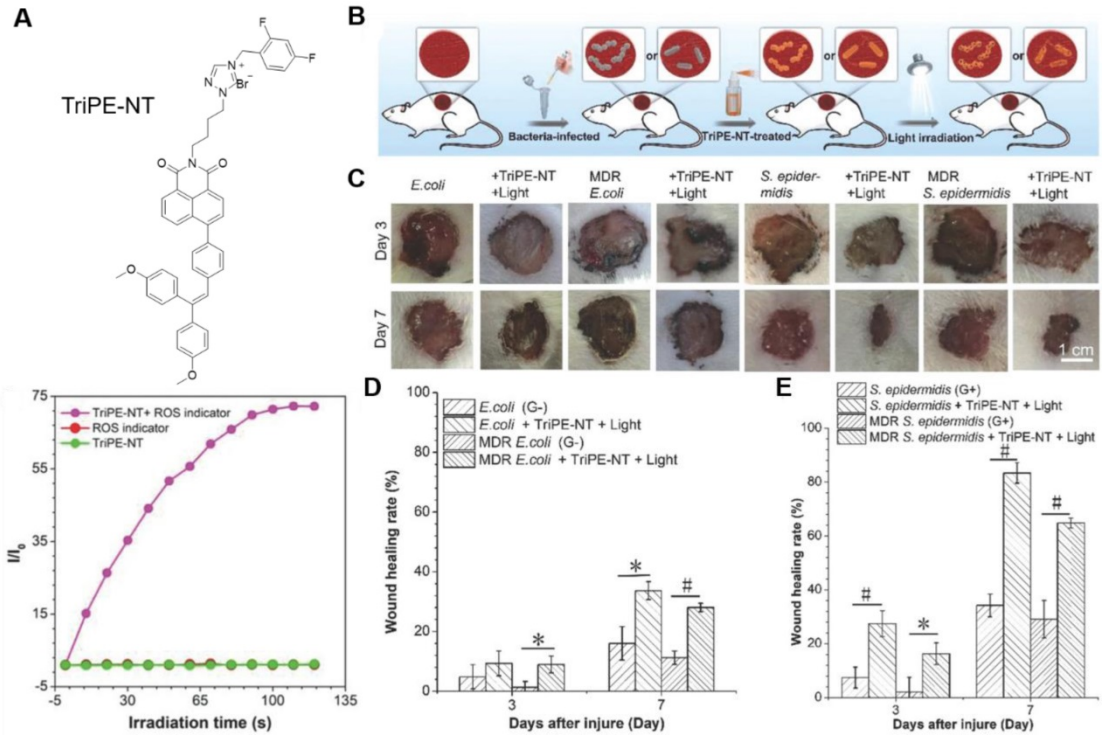

Figure 6. (A) Molecular structure of TriPE-NT and its ROS generation efficiency by plotting of relative PL intensity at 385 nm from DCFH indicator versus the irradiation time. **(B-E)** *In vivo* evaluation of TriPE-NT in treatment of bacteria-infected wounds on rats. **(B)** The cartoon illustrates the process of establishing bacteria-infected full-thickness skin wound models on rats. **(C)** Photographs of wounds treated by TriPE-NT plus white-light irradiation after injury. **(D)** The proportion of the *E. coli*- and MDR *E. coli*-infected wound area after the injury. **(E)** The proportion of the *S. epidermidis*- and MDR *S. epidermidis*-infected wound area after the injury. Reproduced with permission from [78], copyright 2018 Wiley-VCH.

To expand the antimicrobial practice from *in vitro* to *in vivo* level, Tang's group proposed a bifunctional AIEgen, triphenylethylene-naphthalimide triazole (TriPE-NT) (**Figure 6**)[78]. Azoles-substituted naphthalimide (NT) was a common antimicrobial agent, rendering TriPE-NT antibacterial activity. The AIE unit triphenylethylene (TriPE) enabled TriPE-NT to stain both G^+ and G^- bacteria. ROS was efficiently generated under light irradiation, and the antibacterial efficacies against both G^- and G^+ wild-type bacteria as well as MDR bacteria were drastically enhanced. The minimum inhibition concentration (MIC) for TriPE-NT was much lower comparing to a conventional antibiotic, polymyxin. Due to their excellent biocompatibility to mammalian cells, TriPE-NT was further applied in curing *E. coli*-, MDR *E. coli*-, *S. epidermidis*-, and MDR *S. epidermidis*-infected wounds on rats. Under light irradiation, the TriPE-NT could suppress the bacterial infections and promote the wound healing *in vivo* with high efficacy and safety. This study implied the great potential of AIEgens in theranostics of real clinical bacterial infection.

AIEgen-based reactive molecules & responsive molecules for bacterial detection

The multiple charged fluorescent dyes, however, often result in severe alterations of bacterial states by inducing aggregation or metabolic changes in the bacteria. In addition, fluorescent labelling based on electrostatic adsorption is unable to distinguish between live and dead bacteria. To selectively detect the live bacteria, methods based on chemically specific mechanisms have to be developed.

The major component of the bacterial cell wall is peptidoglycan. In G^+ bacterial cell wall, it accounts for 50–80% of the dry weight. And in G^- bacteria, the ratio is 5–20%[79]. Surface polysaccharides possess multiple hydroxyls and are used for binding sites with fluorescent reagents. As study revealed that diols could rapidly conjugate with phenylboronic acid[80], a sensitive AIE-active probe (TPE-2BA), with two phenylboronic acid modified, was designed by Tang's group for bacterial sensing (**Figure 7**, top)[81]. The fluorescence intensity of TPE-2BA in the presence of dead cells was over 12 times higher than that of the living ones, enabling it to differentiate dead and living bacteria. Since TPE-2BA was impermeable to bacterial membrane, that selective imaging of dead bacteria was proved via passing through the compromised membrane and binding to the groove of double-stranded DNA inside the protoplasm, resulting a strong emission. Comparing with commercial DNA staining dyes, TPE-2BA possessed

high brightness, excellent photostability, and could long-term track the bacterial viability even for 3 days with excellent biocompatibility. The feasibility of using TPE-2BA for screening effective bactericides was also demonstrated. However, this TPE-2BA did not stain live bacteria, possibly because that the two phenyl rings without boronic acid were freely rotatable on the bacterial surface. Tang's group therefore synthesized another two similar AIE probes compounds with three and four phenylboronic acid (TriPE-3BA and TPE-4BA), for live bacteria detection (**Figure 7**, below)[37]. The boronic acid-conjugated AIEgens could be used to achieve instant and reliable detection of live bacteria through covalently linking, without causing aggregation and altering the metabolism of live bacteria, which were associated with currently available indicators based on electrostatic interaction. TriPE-3BA and TPE-4BA stained live bacteria and dead bacteria through complexation with cis-diols on bacterial surfaces, with blue color fluorescence emitted out. Comparing to the above TPE-2BA, each of the phenyl rings in TriPE-3BA and TPE-4BA was conjugated with boronic acid, and complexed with the bacterial surface hydroxyl would result in the thorough restriction of all the rotation from the phenyl rings.

Recently, Tang's group reported a catalyst-free click reaction for quick staining and differentiation of bacteria based on an alkyne-active AIEgen (*alkyne*-TPA)[82]. Thanks to the assistance of electron withdrawing group, the nearby alkyne was activated and could directly react with the abundant native groups including amine, thiol, and hydroxyl groups in biomolecules. When encountering bacteria, the active AIEgen could specifically stain G^+ bacteria within 2 min. Whereas, the G^- bacteria showed negligible response even after 30 min coincubation. In contrast to the G^- bacteria that without teichoic acid composition, thick teichoic acid constituted peptidoglycan layers (~20-80 nm), accounting for almost 90% of the whole cell wall, existed in G^+ bacteria with prevalence of free primary amine motif[83]. This difference was supposed to contribute the quick differentiation of G^+ bacteria from G^- bacteria by *alkyne*-TPA, since it could efficiently react with the primary amine. This activated alkyne-based click reaction represents a promising strategy for bacterial detection with advantages throughout simplicity, facility, efficiency and time/cost-saving.

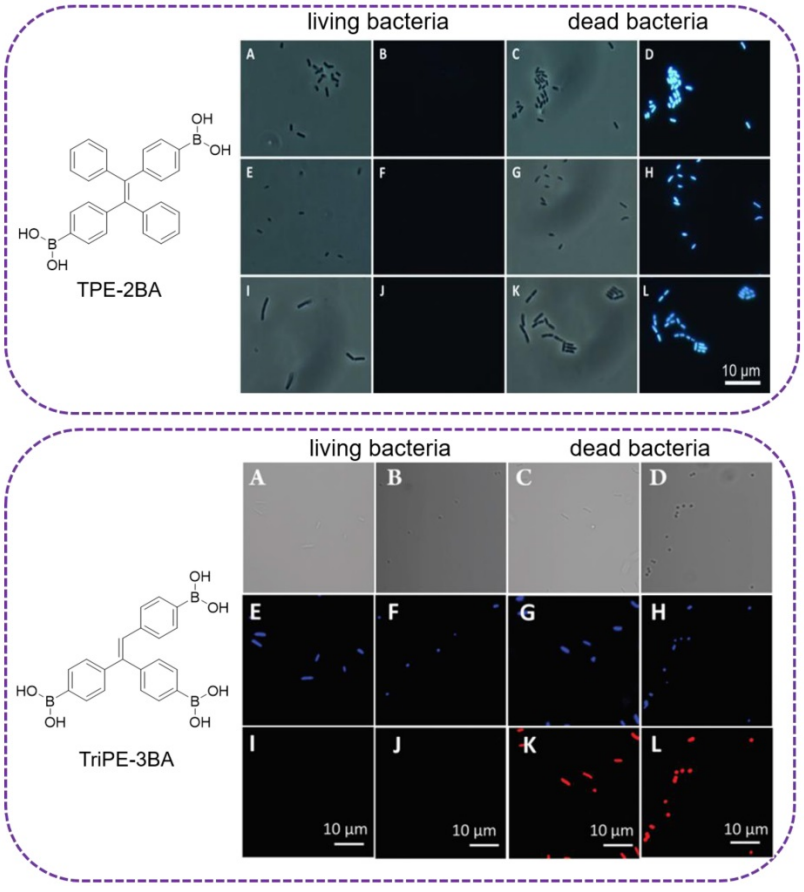

Figure 7. Top: **(A,C,E,G,I,K)** Bright-field and **(B,D,F,H,J,L)** fluorescence images of dead and living **(A-D)** *E. coli*, **(E-H)** *S. epidermidis* and **(I-L)** *B. subtilis* stained with TPE-2BA. Reproduced with permission from [81], copyright 2014 Wiley-VCH. Below: **(A-D)** Bright-field and **(E-L)** fluorescence images of live and dead **(A, E, I, C, G, K)** *E. coli*, **(B, F, J, D, H, L)** *S. epidermidis* stained first with **TriPE-3BA** and then PI. Reproduced with permission from [37], copyright 2018 Royal Society of Chemistry.

Lectins are sugar-recognition proteins that are widely distributed on the surface of bacterial cell wall. Specific sugar-lectin interactions were involved in a number of pathological events, and played a significant role in infection to mammalian cells[84]. Consequently, the sensitive and selective probing of sugar-lectin interactions could offer substantial information for bacterial diagnostics. Considering the polymeric feature of lectins that renders the formation of sugar–lectin complexes with high avidities, glycosyl probes with multivalence are favored for lectin binding. Kumar's group designed a glucose based AIE-active bisacrylamide (Glc-bis) that could target the FimH with multivalences for bacterial detection[85], as the type 1 fimbriae on *E. coli* contained mannose/glucose specific protein FimH, which are uniformly distributed with 100 ~ 400 molecules per cell[86]. Glc-bis could efficiently detect *E. coli* with positive expression of FimH, in concentration range from 1.0×10^6 to 1.7×10^8 cells/mL, with a LOD of 7.3×10^5 cells/mL. What's more, the detection could deliver results in a much shorter period (~ 20 min), comparing to the conventional time-consuming techniques (1-2 days).

Since the emissions of these probes were mainly in the UV or visible light region, which largely hampered their extension towards *in vivo* imaging, Hua's group reported a glyco-AIE probe that can sensitively and selectively detect lectins in the near infrared (NIR) region[87]. Mannosyl and galactosyl diketopyrrolopyrrole (DPP) derivatives were effectively synthesized by the Cu (I)-catalyzed azide-alkyne1.3-dipolar cycloaddition reaction. Upon addition of a selective lectin, the glycosyl DPPs could sharply emit out NIR fluorescence via recognizing the glycosyl moiety of the AIE probe. The detection could be operated in a wide range from 0.25 to 2.0 μM with a nanomolar LOD. With the introduction of graphene oxide (GO) to further decrease the background fluorescence, Hua's group developed another sensitive AIE system for the detection of lectin-sugar interactions in the NIR region[88]. TPA and [1,2,5]Thiadiazolo[3,4-c]pyridine were employed as electron-donor and -acceptor, respectively, to construct the NIR emissive glycosyl probes (glyco-AIE) for specific targeting the lectin on the bacterial membrane. Because of the excellent quenching capability of GO, the sensitivity and selectivity of glyco-AIE probes for the lectin detection could be further improved, with LOD decreased by one order of magnitude. What's more, the glycol-AIE probes showed negligible cytotoxicity to the mammalian cells at concentration even up to 10 μM, indicating the great potential of this chemical tools for the target-specific imaging of lectin over-expressed bacteria *in vivo*.

Sialidases that can specifically hydrolyze the glycosidic bond in sialo-glycoconjugates, are prevalent in bacteria, virus and mammalian cells. Their activities are associated with the pathogenicity of many microorganisms[89]. As a kind of specific enzyme generated by bacterial vaginal infections[90], the detection of sialidases is of great importance for the diagnosis of bacterial vaginosis (BV). According, Wang's group designed a turn-on tetravalent sialic acid-coated TPE luminogen (TPE4S) for highly sensitive and specific detection towards sialidases[91]. The dendrimer TPE4S was equipped via a ''click'' coupling reaction between an alkynyl terminated TPE (TPE4A) and azide-annexed sialic acids. Upon treatment with sialidase to uncage sialic acid moieties, the emission of TPE4A will be rejuvenated with the solubility decrease and aggregates formation. Comparing with the commercially qualitative BVBlue test, TPE4S based fluorescence method presented a pretty better result in accurate classification and quantification of the severity of bacterial vaginosis, after examined in more than 150 real clinical samples from reproductive-age women.

AIEgen derived metal-complexed molecules for bacterial analysis and killing

So far, several positively charged AIEgens have been reported to image and kill bacteria on the basis of electrostatic interactions. To endow the probes with a positive charge, ammonium salts and the zinc (II)-dipicolylamine (ZnDPA) coordination complex are often employed, among which ZnDPA is the most popular as it has a stronger binding affinity with bacteria due to its higher positive charge.

Liu and coworkers reported a multifunctional AIE-Zinc (II)-dipicolylamine (AIE-ZnDPA) probe based on the salicyladazine fluorogen for image-guided photodynamic killing of bacteria (**Figure 8**)[92]. Electrostatic interaction between AIE-ZnDPA and bacteria would lead to the accumulation of AIE-ZnDPA on the bacterial membrane, which was able to activate the AIE plus ESIPT emission via restriction of the intramolecular rotation around the N-N bond and formation of intramolecular hydrogen bonds within the salicyladazine moiety. AIE-ZnDPA could selectively image and kill bacteria, due to the positively charged ZnDPA groups to depolarize the bacterial membrane and phototoxicity through generation of ROS. Whereas, it showed negligible toxicity to the mammalian cells. With significant improvement to this AIE-ZnDPA, Liu's group developed another more advanced metal-complexed AIE probe (TPETH-2Zn) via click chemistry[93]. TPETH-2Zn

could tightly chelate zinc (II) with a nanomolar range K_d value, which was much lower than the previous AIE-ZnDPA. This tight coordination could also result in lower background signal, as less unbound free probes left in the detection system. Rather than the UV region absorbance of AIE-ZnDPA, the TPETH-2Zn was visible-light absorber, which enabled it to produce ROS under white light. As the high abundance of anionic phospholipids on bacterial membrane, TPETH-2Zn could tightly bind to the bacterial surface with AIE fluorescence. The probe could selectively image bacteria over mammalian cells without washing steps. Moreover, under the white light irradiation, pronounced phototoxicity was produced towards killing of both G^+ and G^- bacteria.

As another kind of emissive luminescent material, aggregation-induced phosphorescence (AIP) active iridium (III) complexes were utilized by Panwar's group as potential agents for sensing and inhibition of bacteria [94]. Three tested iridium (III) complexes were found to stain the bacterial cells. They also exhibited antibacterial properties against representative G^+ and G^- bacterial strains. The highest bactericidal potential was observed with MIC values of 4 and 8 mg/mL to G^+ and G^- bacterial, respectively. Preliminary mechanistic studies showed that the DNA binding ability of the iridium (III) complexes was responsible for their antibacterial properties as they were able to penetrate into the bacterial cells and result in the subsequent cell death.

AIEgen modified peptides for bacterial imaging and elimination

As key components of innate immune systems in animal, plant and microorganism, antimicrobial peptides (AMPs) offer immediate and effective defense against pathogenic infections[95]. Most AMPs are cationic and contain 10 ~ 50 amino acids with at least two excess lysine or arginine residues and more than fifty percent of hydrophobic amino acids[96]. They have been used as efficient antimicrobial agents to handle pathogenic infection, especially to the MDR pathogens, due to their broad-spectrum activities and low chance of bacterial resistance[97]. After conjugation with fluorescent AIE reagents, their interaction with anionic bacterial surfaces and the resulted disruption in the pathogen integrity could be monitored in real time.

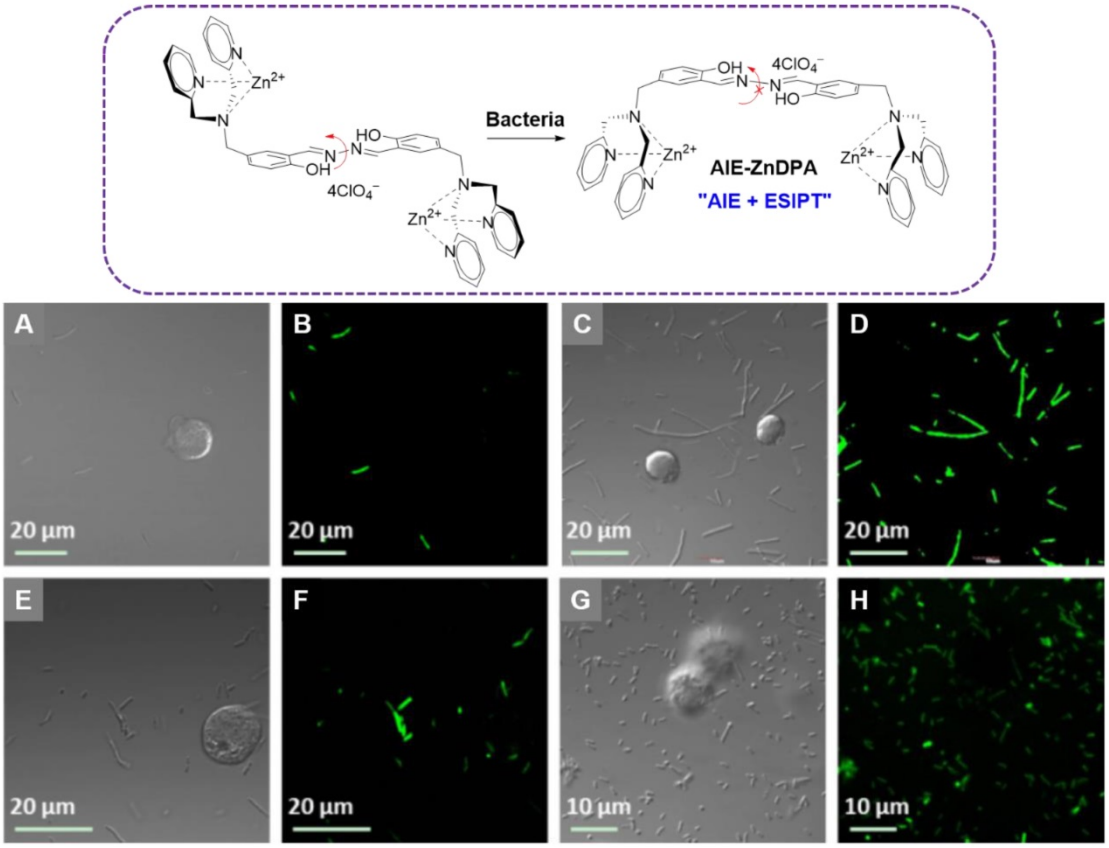

Figure 8. Top: The chemical structure of AIE-ZnDPA, and the schematic illustration of AIE-ZnDPA for selective targeting, imaging, and killing of bacteria over mammalian cells. Below: CLSM images of cells and bacteria incubated with AIE-ZnDPA: **(A, B)** *B. Subtilis* and Jurkat T cells; **(C, D)** *B. subtilis* and K562 cells; **(E, F)** *E. coli* and Jurkat T cells; **(G, H)** *E. coli* and K562 cells. Reproduced with permission from [92], copyright 2015 Wiley-VCH.

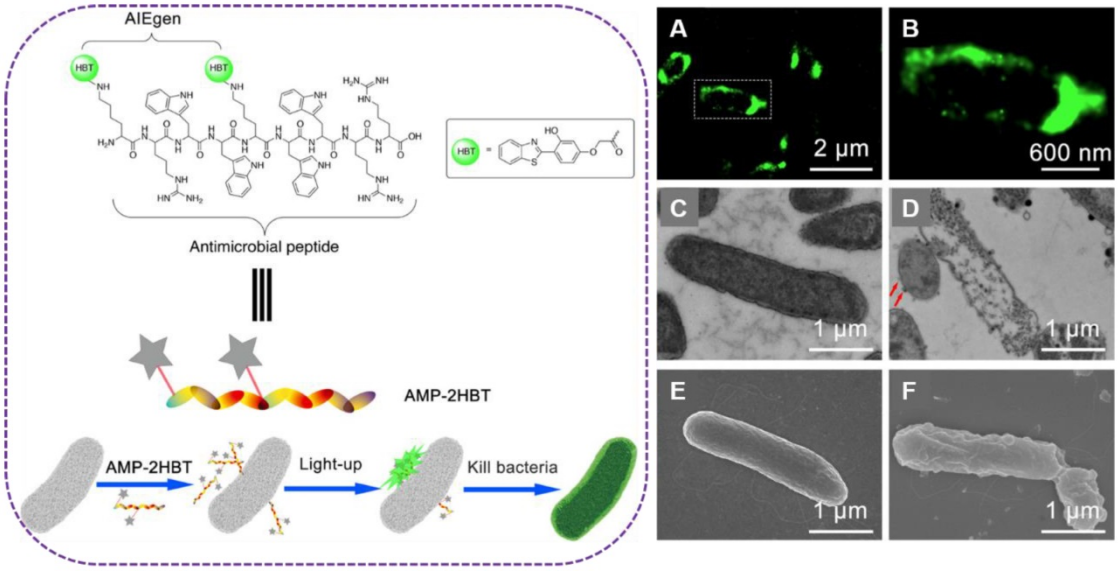

Figure 9. Left: schematic illustration of AMP-2HBT for bacterial imaging and killing. Right: **(A,B)** Super-resolution fluorescence images of *E. coli* after treatment with AMP-2HBT. The TEM images of *E. coli* before **(C)** and after **(D)** treatment with AMP-2HBT. The bubbles protruded from the cell membrane were indicated by red arrows. The SEM images of *E. coli* before **(E)** and after **(F)** treatment with AMP-2HBT. Reproduced with permission from [99], copyright 2018 American Chemical Society.

Xu's group synthesized TPE-containing AMP (TPE-AMP) via thiol-ene conjugation between a cysteine-terminated AMP (CysHHC10, Cys-Lys-Arg-Trp-Trp-Lys-Trp-Ile-Arg-Trp-NH_2) and a TPE derivative [98]. TPE-AMP showed a pretty higher affinity for the G^+ bacterial membranes, as the arginine and tryptophan residues favored to insert into G^+ bacterial membranes. CysHHC10 exhibited strong antimicrobial properties against both G^+ and G^- bacteria. Upon conjugation with TPEMA, the resulting TPE-AMP also exhibited similar antimicrobial properties. The MIC values of TPE-AMP towards G^+ and G^- bacteria still maintained at micromolar level. Further, TPE-AMP exhibited negligible toxicity *in vivo*, indicating its potential in treatment of the infected tissues in animal infection models.

In order to investigate the bactericidal mechanisms of AMPs, Tang's group developed an AIE-active probe AMP-2HBT through decorating antimicrobial peptides (HHC36 with sequence of KRWWKWWRR) with AIEgen (2-(2-hydroxyphenyl)-benzothiazole, HBT) (**Figure 9**)[99]. This AIE-active probe exhibited free self-quenching, high signal-to-noise ratio, strong photostability and could be used for real-time monitoring of the binding process between antimicrobial peptide HHC36 and bacteria in a wash-free manner. The AIEgen decorated on HHC36 peptide did not compromise the bactericidal activity. Moreover, though real-time fluorescent imaging, the mechanism of excellent bactericidal activity of HHC36 peptide could be ascribed to its aggregation on the bacterial membrane and disruption of the membrane structure, which caused the flowing out of inner nucleic acids or proteins.

Among the glycopeptide antibiotics, vancomycin (Van) with specific binding affinity to peptidoglycan sequence N-acyl-D-Ala-D-Ala presented on G^+ bacterial cell walls have been widely used for the treatment of G^+ bacteria. However, the emergence of vancomycin resistant *Enterococcus* (VRE) leads to largely decreased binding affinity (over 1000-fold) for Van, which has caused serious infection problems. Liu's group report a novel light-up AMP via conjugation of Van with AIEgen to yield AIE-2Van probe for image-guided PDI of bacteria[100]. AIE-2Van could specifically image G^+ bacterium and VRE bacteria, with enhanced red fluorescence emission at 650 nm. Similar to the antibiotic property of Van itself, AIE-2Van showed similar MIC activity against G^+ bacteria in the dark, and the MIC values decreased significantly under white light irradiation. Enhancement in killing effect was achieved on the VRE strains from PDI effect. Binding of AIE-2Van to G^+ bacterium in the dark led to a rough surface and a damaged membrane, and light irradiation further increased the damage level with fragmentations, swelling, splitting and collapse to their cell walls. However, negligible effects were found towards G^- bacteria no matter white light irradiation or not. As GO is an effective quencher for many fluorophores, there is a unique opportunity to combine GO with AIEgens for designing of light-up bioprobes with minimum background noise. Liu's group, therefore, introduced GO to detect bacteria

with AIE-2Van[101]. In the presence of GO, the probe incubated with G^+ bacteria showed strong turn-on fluorescence. Other bacteria including representative G^- and VRE strands, could only induce faint fluorescence emission, indicating the perfect selectivity towards G^+ bacteria.

AIEgen constituted polymers for bacterial monitoring and killing

Unlike antibiotics from small molecule that disrupt specific physiological processes during pathogen growth or proliferation, macromolecular biocides such as polymers usually implement their activities through noncovalent interactions with microbes, thus rarely causing resistance.

In many scenarios, microbes to be detected are unknown or may not be previously identified, so that probes grafted with recognizing ligands such as carbohydrates or antibodies might not be effective. In order to expand the scope of bacterial detection means, it is thus reasonable to develop fluorescent macromolecular probes that are responsive to negatively charged surfaces, given that most bacteria possess negatively charged surfaces. Liu's group designed a system capable of both bacterial detection and inhibition, where polyion complex (PIC) micelles were constructed from negatively charged TPE sulfonate derivatives and cationic diblock copolymers, PEO-*b*-PQDMA[102]. Upon contacting with bacteria, the PIC system disintegrated presumably due to competitive binding of polycation blocks with negatively charged bacterial surfaces. This process would release free TPE derivatives and be accompanied with fluorescence emission quenching due to the loss of AIE effect, which could serve as a real-time modality for microbial detection. Meanwhile, cationic PQDMA block also exhibited antibacterial effects against G^- and G^+ bacteria strains, with sharp decrease in CFU. By tuning the charge density and chain length of cationic PQDMA block, optimal performance against G^- bacteria was achieved with a LOD of 5.5×10^4 CFU/mL and MIC of 19.7 mg/mL.

Based on one of the macromolecular antimicrobial peptide mimics, P(DMA-*co*-BMA), Liu's group advanced a new amphiphilic star copolymer, TPE-*star*-P(DMA-*co*-BMA-*co*-*Gd*) for bacteria detection and inhibition (**Figure 10**)[103]. The platform with AIE feature was consisting of a TPE core and bacteria-binding and amphiphilic/cationic P(DMA-*co*-BMA-*co*-*Gd*) arms, where *Gd* was T1-type magnetic resonance imaging (MRI) contrast agent, DOTA-*Gd*. The star copolymer could act as fluorescence and MRI dual-modality sensing probes for *E. coli* detection with LODs of ~8.5×10^5 CFU/mL and ~5×10^3 CFU/mL, respectively. As one of the macromolecular AMP mimics, copolymer S-3 showed the highest antibacterial activity as well as hemolysis ability, with MIC values of ~0.1 and 30 μg/mL against *P. aeruginosa* and *S. aureus* bacteria strains, respectively. Further quaternization of this star copolymer could significantly enhance its selectivity towards microbes over mammal cells, as biocompatibility to human red blood quantitatively increased by more than 4 orders of magnitude.

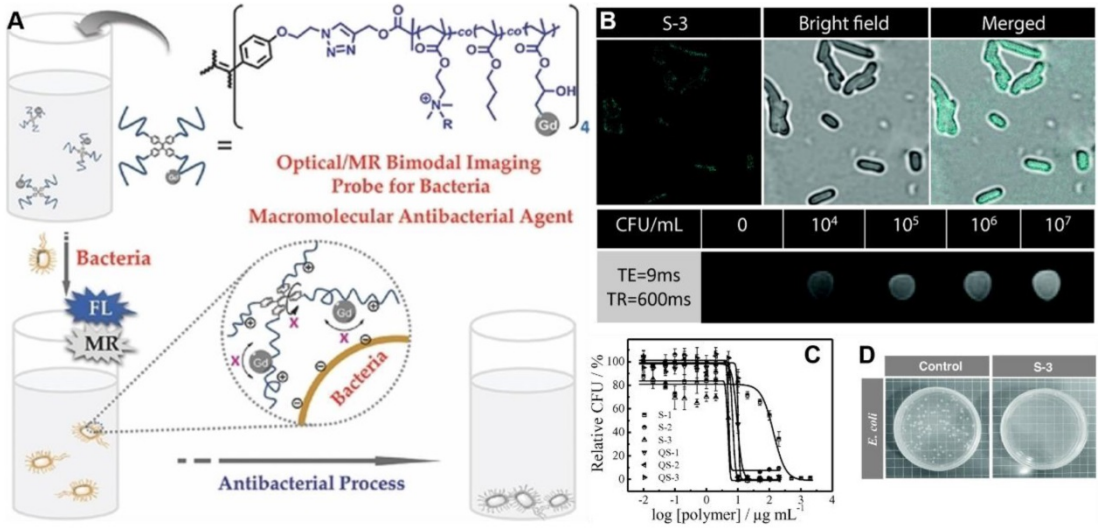

Figure 10. (A) Schematic illustration of fluorometric/magnetic resonance bimodal detection of bacteria based on amphiphilic star copolymers. **(B)** Confocal laser scanning microscopy images recorded for *E. coli* upon S-3 star copolymer labeling and T_1-weighted MRI images in the presence of varying concentrations of *E. coli* cells. **(C)** Survival rate of *E. coli* as a function of star copolymer concentrations. **(D)** Antibacterial tests with *E. coli* strains. Reproduced with permission from [103], copyright 2014 Wiley-VCH.

As mimic antimicrobial AMPs, peptide polymers could offer good biocompatibility. Wang's group thus designed nanoengineered peptide-grafted hyperbranched polymers (NPGHPs) for bacterial killing [104]. In the structure of NPGHPs, H-PAMAM containing AIEgen was used as an initiator, and lysine/valine monomers were randomly grafted onto the H-PAMAM core. This mimic AMPs could be large-scale synthesized with low cost. Apart from their capability of sensitive detection of bacterial, with a LOD down to 1×10^4 CFU/mL, the hyperbranched architecture of NPGHPs with the high local concentration of charges can significantly enhance their antimicrobial activity against both G^+ and G^- bacteria. Most importantly, NPGHPs could act as fluorescent probes to monitor the antimicrobial process that included aggregation on membrane, membrane shape changing, fragmentation, and eventual break down, in a real time manner. In addition, NPGHPs showed good biocompatibility in cytotoxicity and hemolysis studies.

To introduce extra PDI effect to the AIE featured polymeric antimicrobial material, Zhang's group synthesized a multiple-cation charged AIE-active polymer, DBPE-DBO[105]. It exhibited enhanced quantum yield and red-shifted emission wavelength comparing to the DBPE precursor. DBPE-DBO possessed multiple interaction points to contact with bacteria, and the hydrophobic alkyl chains were able to intercalate into the membrane of the bacteria. Due to the combination of dark toxicity from positively charged polymers, the phototoxicity from generation of singlet oxygen, and the AIE-active fluorescence, DBPE-DBO could be employed for efficient bacterial targeting, imaging and killing, as more than 99% of both G^+ and G^- bacteria were eliminated under 1 h room light irradiation. What's more, DBPE-DBO could selectively kill bacteria but was harmless to normal mammalian cells.

Biomarkers on the bacterial surface are accessible for bacteria detection through antibody-antigen recognitions or other specific ligand-receptor interactions. As mentioned above, FimH over-expressed on bacterial membrane is a two-domain adhesion protein at the end of a fimbria. Whereas, the weakness of mannose-FimH interactions requires several mannose molecules to bind simultaneously with a single *E. coli* cell for a stable complex formation. As an efficient processing method, electrospinning was applied by Li's group for synthesis of poly styrene-*co*-maleic anhydride (PSMA) fibers that conjugated with mannose and TPE-Man for *E. coli* detection[106]. They exhibited advantages including the high grafting capabilities of ultrafine fibers and the highly porous structure of the fibrous mat to tightly entrap bacterial cells. The specific and multivalent binding between mannose grafts on PSMA fibers and FimH proteins from *E. coli* led to an efficient "turn-on" fluorescence signal. Comparing to the hexamethylenediamine or poly(ethylene imine) spacers for mannose grafting, this electrospun polymer showed more sensitive fluorescence signal, lower fluorescence background, wider space for bacteria binding and higher anti-interference capability, as the detection range against *E. coli* was as wide as from 10^2 to 10^5 CFU/mL, with a LOD down to 10^2 CFU/mL.

As bacteria express large amounts of alkaline phosphatase (ALP) that dominantly located in the periplasmic area of the bacterial surface, Park's group designed an ALP catalyzed colorimetric method using a surface-adsorbing biosensor for bacterial detection and killing[107]. The phosphorylated fluorescent probe 2-hydroxychalcone (HCAP) was conjugated with an adhesive cationic polymer PVP. It could be used in solid-phase detection assay after the HCAP-PVPs were functionalized with catechol moieties to increase their adhesiveness to solid surfaces. Upon introduction of bacteria, the phosphate group inside the HCAP was cleaved by endogenous ALP and activated the ESIPT and AIE processes simultaneously, inducing the ratiometric change in emission color. This biosensor could detect bacteria over a wide range (10^1-10^7 CFU/mL). Outperforming to PCR and ELISA, sample pre-treatment with specific chemicals was not required in this ALP mediated fluorescent method. Moreover, the quaternary ammonium of dodecane in this system displayed efficient antibacterial activity, enabling HCAP-PVPs to act as dual sensor and killing materials.

AIE featured nanoparticles for bacterial theranostics

Nanoparticles hold great potential for both antibacterial application and rapid detection of pathogens due to their unique physicochemical properties. Especially, the large surface area of nanomaterials can enhance their interactions with microbes. Also, nanoparticles are believed to be more effective and less likely to induce resistance in most MDR cases, since their antimicrobial properties involve direct contact with the outside membrane, instead of penetrating into the pathogens. Molecular self-assembly is a spontaneous agglomeration of individual components into well-ordered structures with the aid of non-covalent interactions including electrostatic interaction, hydrogen bonding, π–π interaction, hydrophobic effect, etc. As a prototype of nanoparticles, AIE nanodots could be prepared easily through solvent polarity tuning, and the formed

nanoaggregate possesses excellent photo-stability, biocompatibility and flexibility in molecular and structure design. Comparing to the planar chromophores that are prone to form bulk crystals, the nanosized aggregates from AIEgen self-assembly present pretty better stability, as supramolecular interactions are often participated in their formations.

Outperforming to the one-photon excited fluorophores, two-photon fluorescent (TPFL) probes exhibit advantages including slower photobleaching, deeper penetration depth, lower background signal and phototoxicity via use of NIR excitation. Since organic nanoparticles are mostly prominent agents with TPFL, a series AIE nanodots that prepared from TPE-based nitrogen (N)-containing heterocycle with pronounced TPFL, were reported by Jiang's group [108]. The AIE dots exhibited excellent TPFL performances in the sensitive detection of bacteria. In the molecular structure of AIEgen, TPE unit was employed as an electron donor with AIE-activity, and pyridine, quinoline and acridine were electron acceptor for tuning the emission colors and interactions with bacteria for their positive charges. The AIE nanodots could be facilely prepared by adding DMSO solutions of these compounds into aqueous solution. They can image G^+ and G^- bacteria via different TPFL signals. Compared to the conventional one-photon microscope, the TPFL signal exhibits advantages in reduced substrate autofluorescence and self-absorption, as well as deeper tissue penetration.

Yan and coworker reported a modular formulation of theranostic pure nanodrugs (PNDs) based on fluoroquinolones[109]. They were propeller-shaped, and upon precipitation into water, readily assembled into stable nanoaggregates with AIE activity. The formed nanoaggregates could fluorescently image bacteria with high efficiency. On the other hand, fluoroquinolones are among the most prescribed antibiotics for the treatment of various infections. Their broad-spectrum efficacy is associated with the inhibition of DNA replication and repair. Comparing to other nanotherapeutics that were often drug carrier dependent, PNDs were composed entirely of the drug molecule, and the drug-loading efficiency could reach 100%. Thus, aggregation-enhanced antibacterial activity could be achieved from the PNDs. They lowered the MIC against both sensitive and resistant *E. coli* by more than one order of magnitude, due to the increasing in local drug concentration with nanoaggregates colocalization, and the enhanced uptake efficiency when delivered in the nanosized particles.

As the bacterial infection frequently occurred in the tissue or organism level, it is necessary to extend the specific detection and killing of bacteria to *in vivo* practice. Based on the capability of chemical sensing or imaging of bacteria from the nanoparticle self-assembled by tetraphenyl imidazole derivatives, Zeng's group designed an AIE-active tetraphenyl imidazole molecule (TPTP) and applied it to bacterial infection treatment *in vivo*[110]. TPIP contained three components: (1) the alkyl chain that could regulate the spatial position of the positive charge and improve the biocompatibility, (2) the imidazole that was used as both AIEgen and bactericide, and (3) the pyridinium that acted as a hydrophilic terminal group and antimicrobial moiety. In aqueous solution, TPIP could self-assemble into fluorescent organic nanoparticles (FONs) with AIE activity. The FONs exhibited good photostability, high water solubility and could selectively image G^+ bacteria without washing process. The detection range was from 3×10^7 to 3×10^8 CFU/mL, with a LOD of 5.2×10^5 CFU/mL. TPIP-FONs also displayed excellent antibacterial activity against G^+ bacteria *in vitro* with MIC value of 2.0 μg/mL. Due to the electrostatic and hydrophobic interactions from the positively-charged pyridinium and alkyl chain of TPIP-FONs, respectively, the cell walls of G^+ bacteria became wrinkled and damaged, with the appearance of outer membrane vesicles and leakage of intracellular contents. Furthermore, TPIP-FONs exhibited intrinsic biocompatibility with mammalian cells. In the infectious sites *in vivo*, TPIP-FONs presented excellent antibacterial efficacy and could reduce the bacteria colonies by more than 85%, with negligible change happened in the control group.

Metal–organic frameworks (MOFs) have been considered as a promising candidate for drug delivery, because of their excellent storage capacities, easy body clearance and low cytotoxicity. More importantly, the versatile chemical properties of MOFs endow them with the capability to regulate the delivery of drugs, as triggered by various external stimuli. Taking advantage of the MOF-based MIL-100 (Fe) nanoparticles, Liu's group reported a two-step strategy to achieve *in vivo* metabolic labeling and image-guided antibacterial therapy (**Figure 11**)[111]. MIL-100 (Fe) nanoparticles were first formulated as d-AzAla carriers, which could be degraded in the presence of H_2O_2. Consequently, the encapsulated d-AzAla could be released in H_2O_2 oversecreted inflammatory region. D-AzAla was then specifically taken up by the bacteria and integrated into the cell walls of bacteria. Ultrasmall US-TPETM nanoparticles with intense AIE-active NIR fluorescence and strong photosensitizing capability were subsequently injected to react with the modified bacteria through *in vivo* click chemistry. With white light-assisted

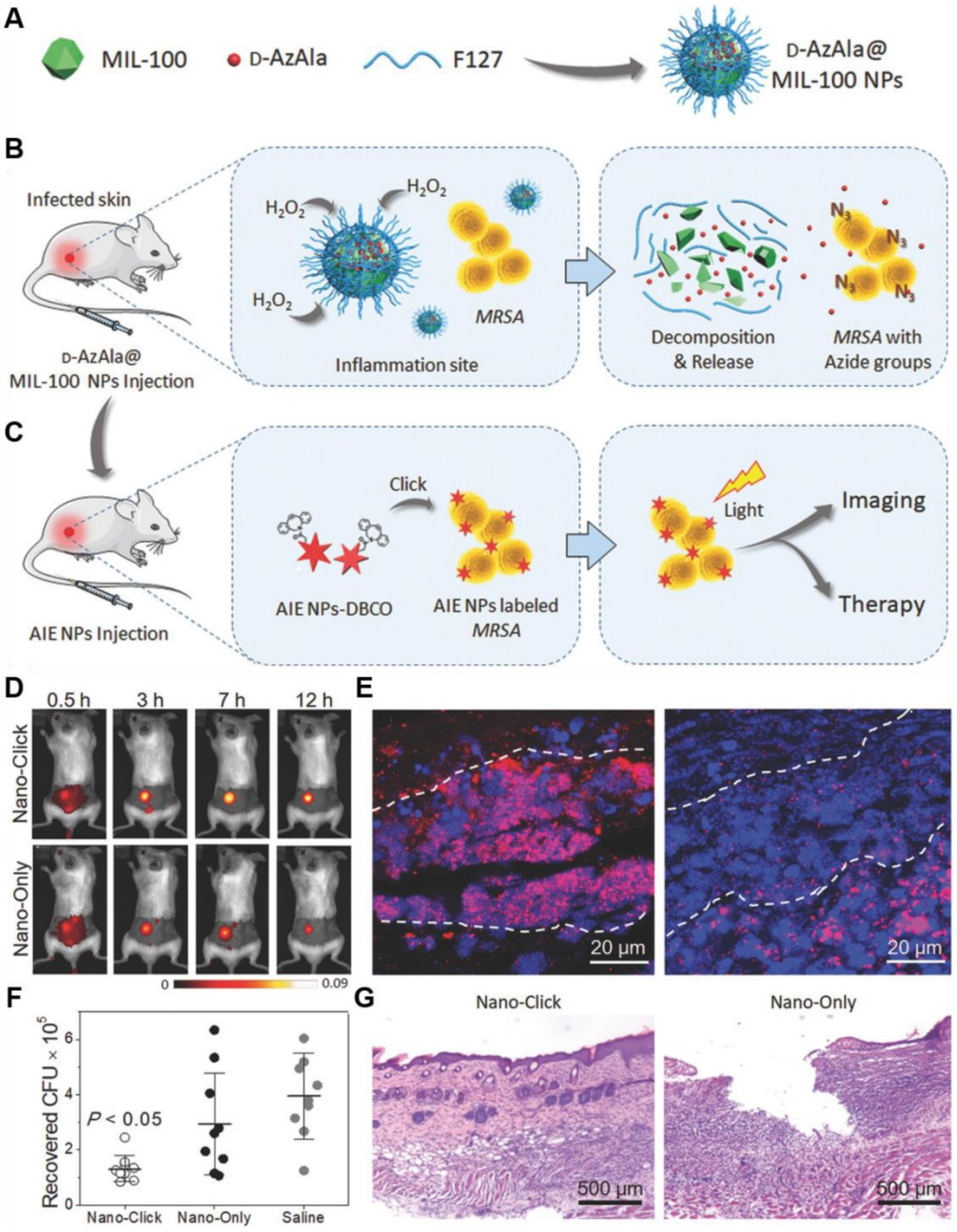

Figure 11. (A-C) Schematic illustration of the proposed strategy of bacteria diagnosis and therapy by the H_2O_2-responsive MOFs. **(A)** The synthesis of D-AzAla@MIL-100 (Fe) NPs. **(B)** Accumulation, decomposition and expression of D-AzAla on the bacterial wall. **(C)** Binding of ultrasmall US-TPETM NPs with bacteria. **(D-G)** *In vivo* bacteria killing using US-TPETM NPs. **(D)** *In vivo* fluorescence images of bacteria-bearing mice. **(E)** Fluorescence images of the infected skin slices of mice pretreated with D-AzAla@MIL-100 (Fe) NPs. **(F)** Bacteria CFU recovered from the infected skin. **(G)** Hemotoxylin and eosin stain of the infected skin slices. Reproduced with permission from [111], copyright 2018 Wiley-VCH.

photodynamic therapy, bacteria on the infected tissue can be efficiently eliminated. This powerful metabolic biomolecular labeling technology with the NIR emissive photosensitizer showed great potential for in situ pathogen detection and killing in *in vivo* level.

AIE featured host-guest systems for bacterial assay

Nowadays, host-guest based supramolecular chemistry has brought significant improvements to the research in chemical, biological and material science. During the past decades, supramolecular methods as new analytical tools have received increasing attention. As exhibiting different interaction manners with pathogen surfaces before and after assembly, supramolecular complexes are widely applied in discrimination and identification of pathogen with rapid and facile conveniences. In order to further endow the cationic polymer complexed

supramolecular system with antimicrobial function, Gao's group developed an AIE-featured multifunctional host-guest system (PEI-CD-Arg-TPEDB)[112]. It composed AIEgen (4,4'-(1,2-diphenylethene-1,2-diyl) bis(1,4-phenylene)diboronic acid, TPEDB) that linked to cyclodextrin (CD) via host-guest interaction, and polyethyleneimine (PEI) which was covalently modified by arginine (Arg). TPEDB was capable of fluorescently identification and long-term surveillance of G^+ and G^- bacteria for over 72 h without washing process. The Arg components could extensively suppress bacterial activity via electrostatic adhesion to the bacterial surface and disruption of Ca^{2+} salt bridges. Furthermore, the production of ROS by PEI-CD-Arg-TPEDB increased the antimicrobial effect, and the MIC decreased more than one order of magnitude toward both G^+ and G^- bacteria. Moreover, it did not give rise to any resistance after repeated use on both G^+ and G^- bacteria.

To circumvent the undesirable cytotoxicity of the above used cationic PEI polymer, Gao's group further designed a multifunctional supramolecular nanomaterial (**Figure 12**). Based on mesoporous silica nanoparticles (MSNs) that loaded with amoxicillin (AMO), the supramolecular nanostructures were fabricated through layer-by-layer assembly of 1,2-ethanediamine modified polyglycerol methacrylate (PGEDA), cucurbit[7]uril (CB[7]) and AIE-active TPE carboxylate derivatives (TPE-$(COOH)_4$)[113]. In the presence of bacteria, the competitive binding of negatively charged bacteria to the positively charged PGEDA would lead to the quenching of fluorescence emission due to the disassembly of TPE-$(COOH)_4$. The bacteria could be detected with a LOD of 2.5×10^6 CFU/mL through the change in fluorescence signal. More significantly, this supramolecular nanomaterial possessed controllable antibacterial activity that could be regulated by the simple supramolecular assembly and disassembly processes. In detail, upon adding AD, a more stable inclusion complex AD⊂CB[7] formed and PGEDA was liberated through competitive replacement, resulting the release of AMO and much higher antibacterial ability of nanoassembly. Comparing to MSN-PGEDA CB[7]-TPE alone, MSN-PGEDA-CB[7]-TPE with AD exhibited much higher killing efficiency toward both G^+ and G^- bacteria. Furthermore, negligible cytotoxicity was observed towards mammalian cells.

Fungal discrimination and killing

Fungi are important eukaryotic organisms of ecosystem. They are capable of causing various diseases such as respiratory problems. Fungi grow at enormous rate when suitable conditions such as humidity and temperature appear. More seriously, they can survive in extreme environmental conditions for their spore-type propagations.

Small molecules for fungal differentiation and elimination

Sivasudha's group reported a pyrene containing Schiff base molecule, namely 4-((pyren-1-ylmethylene)amino)phenol (KB-1) for fungi killing[114]. The fluorescence of this molecule was

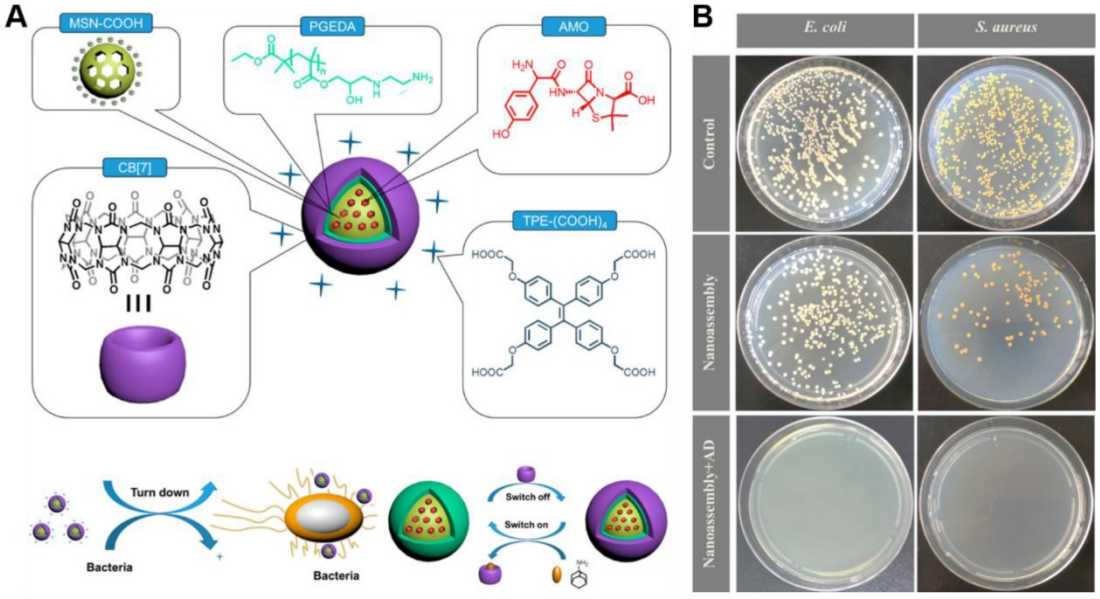

Figure 12. (A) Schematic representation of nanoassembly and possible mechanism for bacterial detection and controllable inhibition. **(B)** CFU for *S. aureus* and *E. coli* treated with nanoassembly before and after addition of AD on agar plate. Reproduced with permission from [113], copyright 2017 American Chemical Society.

completely quenched due to photoinduced electron transfer (PET). With hydrogen bonding interaction of imine donor with water, the PET could be suppressed and the fluorescence of KB-1 could be turned on for its AIE property. Apart from its antibacterial activity towards G^+ and G^- bacteria, KB-1 possessed efficient antifungal capability towards *C. albicans*. The fluorescence of KB-1 was used to probe the fungi attributed to the interaction between the OH group in the active site of KB-1 and the membrane proteins of microbial walls. As a result, the cell membrane permeability increased, and the intra cellular components leaked out, leading to the death of fungi. Singh's group from India found that chromone S1 with both ESIPT and aggregation-induced emission enhancement (AIEE) property, could also be applied for fungi killing[115]. The supramolecular aggregates of S1 underwent disaggregation in the presence of Cu^{2+} with decrease in fluorescence intensity. It could reassemble after Cu^{2+} were chelated by CN^- due to the higher affinity, with recovery of the AIEE fluorescence. Interestingly, both S1 and S1-Cu^{2+} complex showed excellent antimicrobial activities against two fungal strands, in which, the metal complex exhibited much higher inhibitory effect owning to its metal activity.

Meanwhile, the discrimination of living pathogens, such as G^+, G^- bacteria and special fungi, are of more practical significance for the promotion of diagnosis and treatment. As the difference in the components of microbial wall, Tang's group applied the aforementioned M1-DPAN for the discrimination of G^+ from other bacteria and fungus (**Figure 13**)[71]. Both of the components and structure of cell walls decided the selective discrimination of G^+. The binding affinity of M1-DPAN toward lipoteichoic acid (LTA) (K_b = 2.05×10^6 M^{-1}) was 3 orders of magnitude higher than that of LPS, as LTA and LPS were specific and major components on the wall of G^+ and G^-, respectively. The alkalinity and morpholine groups in M1-DPAN played crucial roles in discrimination of G^+ from fungi, as the counterpart molecules without morpholine or alkalinity failed in the specific staining of G^+ bacteria.

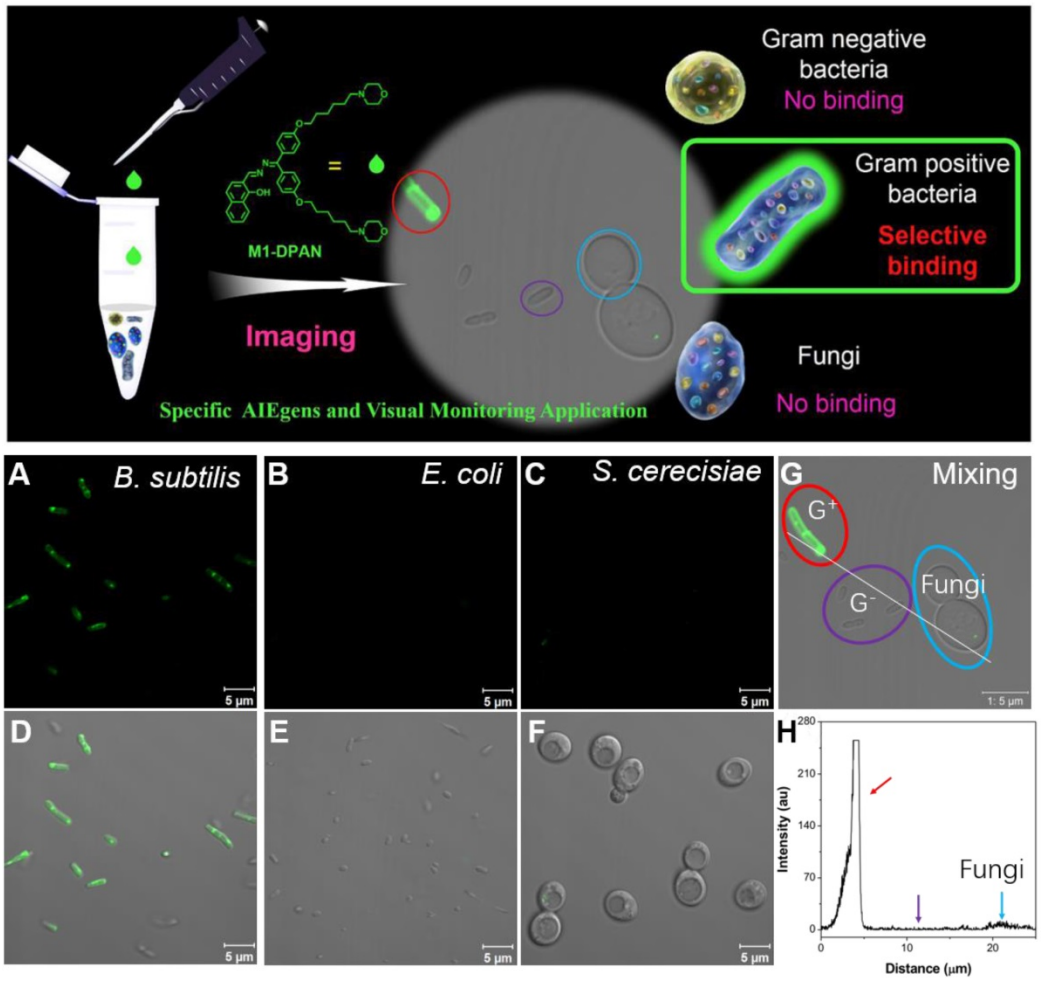

Figure 13. Top: schematic illumination of G^+ specific discrimination by M1-DPAN. Below: the adsorption of M1-DPAN on the surfaces of *B. subtilis* **(A, D)**, *E. coli* **(B, E)**, *S. cerecisiae* **(C, G)**, The CLSM image **(G)** and line series analysis **(H)** of mixture of *B. subtilis*, *P. aeruginosa* and *S. cerecisiae* with M1-DPAN. *B. subtilis* is denoted by a red circle, *P. aeruginosa* is denoted by a purple circle, and *S. cerecisiae* is denoted by a cyan circle. Reproduced with permission from [71], copyright 2018 Elsevier.

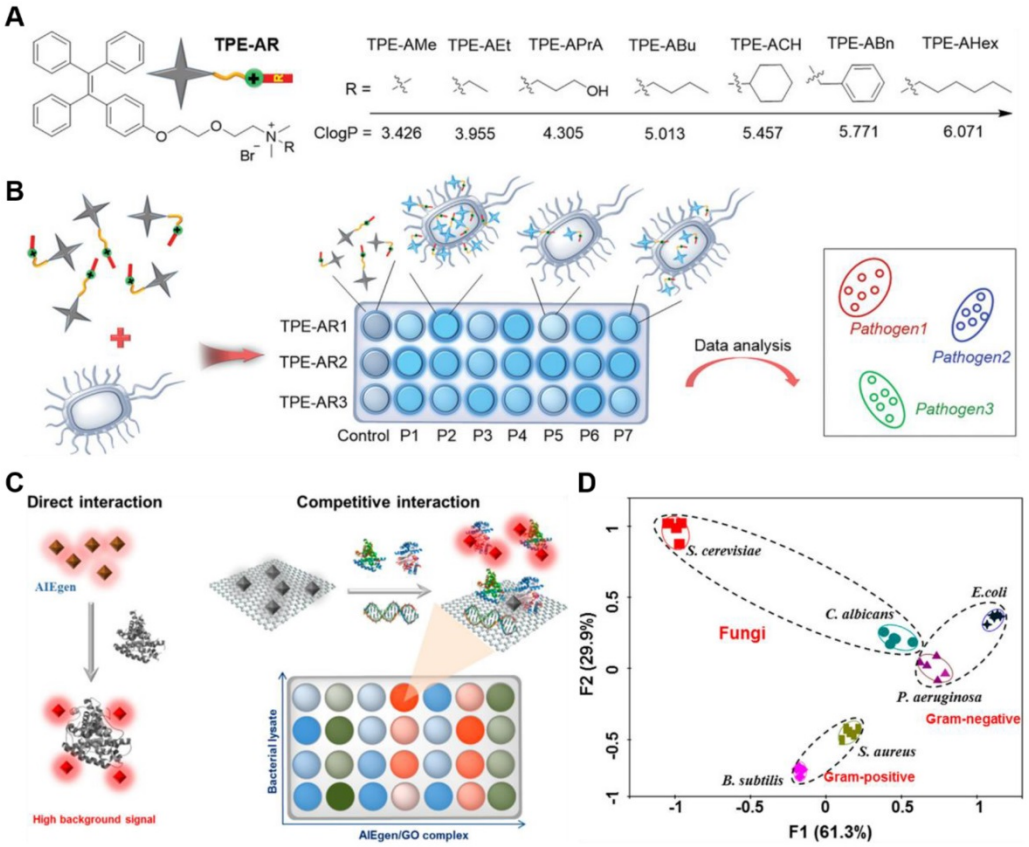

Figure 14. (A) Structure of TPE-ARs with various ClogP values. **(B)** Schematic illustration of a sensor array composed of three TPE-ARs to achieve pathogen identification. P1–P7 represent seven kinds of pathogens. Reproduced with permission from [117], copyright 2018 Wiley-VCH. **(C)** Schematic illustration of two ways of interaction in constructing a sensor array. The left represents the direct interaction between AIEgens and biomolecules, and the right demonstrates the competitive interaction among AIEgen, biomolecules and GO. **(D)** Principal component analysis results of the formed patterns generated from six microbial lysates. Reproduced with permission from [119], copyright 2018 American Chemical Society.

Array assay for fungal discrimination

Analytical strategy based on sensor arrays is conducive to high-throughput screening and can be used to identify multiple analytes simultaneously, by using a number of non-specific or cross-reactive probes[8]. Following statistical analysis, signal patterns can be isolated and used to unambiguously identify the unknown analytes. Over the past two decades, various arrays for the identification of microorganism have been reported. These often employ fluorescence methods, owing to their good sensitivities and versatile signal output as well as easy to read out.

Jiang and Zhang's group developed fluorescent arrays (F-arrays) for the rapid and efficient identification of various microbes using five AIE-active probes[116]. The molecules were endowed with different charged groups and hydrophobic properties, resulting various interactions with the bacteria and different types of output fluorescent signals. The collective fluorescent signals were used to construct sensor arrays for identification of various fungi, G^+ and G^- bacteria without washing process. Through professional statistical analysis, eight kinds of pathogen were classified and identified with 100% accuracy. What's more, 11 out of 12 unknown microbial samples randomly from the above eight species were determined with an accuracy of as high as 91.7%. Together, this method featured high-throughput, easy-to-perform, time-saving and high signal-to-noise ratio of fluorescence signal that could be automatically recorded by flow cytometry.

As the fabrication of sensor arrays to identify pathogen required diverse fluorescent responses presented when one strain incubated with different AIEgens and different strains incubated with the same AIEgen, Tang's group reported seven types of TPE derivatives for construction of 14 kinds of competent sensor arrays to detect and discriminate fungi from various pathogens (**Figure 14a,b**)[117]. Each sensor array consisted of three TPE-based AIEgens that bearing common cationic ammonium group but different hydrophobic substitutions. Tunable log*P* (*n*-octanol/water partition coefficient) values from 3.426 to 6.071 were endowed to guarantee the different multivalent interactions with pathogens. With the log*P* value increasing, the affinity of

TPE-ARs toward G^+ bacteria and fungi was gradually weakened and changed into the higher affinity to G^- bacteria. Since each sensor array afforded a unique fluorescence response pattern for different pathogens, these sensor arrays can identify seven different pathogens, including G^+ and G^- bacteria as well as their MDR counterparts with nearly 100% accuracy, with the aid of special statistical analysis. Furthermore, blends of 8 kinds of pathogens could also be identified with 100% accuracy.

Different from previous pattern based microbial entity identification, microbial lysates instead of intact microbes could also be applied as analytical target[118]. They could eliminate the potential health threats from the living pathogens, and provide information about the inside composition of microbes, which was helpful to distinguish different strains of bacteria from the same family. However, microbes contained large number of molecular species, such as saccharides, peptides, and nucleic acids, and over 70% percent of the total peptide content was identical that might interfere the identification result. Therefore, Tang's group constructed a GO assisted fluorescent sensor array using seven kinds of AIEgens with varying charges for microbial lysate identification (**Figure 14c,d**)[119]. The combination of AIEgen with GO not only reduced the background signal but also induced the competition interactions among AIEgen, microbial lysates and GO, which could highly improve the discrimination ability of the sensor array. Nucleic acids and proteins were founded to determine the recovery of the fluorescent signal in the sensor array, in which biomolecular species rather than biomolecular concentration played the key role. The sensor array exhibited ultrahigh sensitivity, with LOD of 10^4/mL for fungus *C. albicans*. What's more, two fungi from four classes of G^+ and G^- bacteria were differentiated and identified with 100% accuracy and the fluorescent patterns could maintain for longer than 12 h.

AIEgen-based viral immunoassay platform

Emerging and re-emerging of viral infectious pathogens severely threaten human health and have become one of the major public health concerns. Developing sensitive and accurate methods for virus clinical diagnosis is of great significance, especially for the early stage of infection, to prevent virus spread and disease outbreaks. Tang's group reported an ultrasensitive immunoassay platform for various kinds of virion detection (**Figure 15**)[120]. It was featured with fluorescence and plasmonic colorimetry composed dual-modality read-out based on a water-soluble multifunctional AIEgen (TPE-APP) with ALP enzymatic cleavage sites. After the immunocapture of target virus, the ALP was coupled to the ELISA sandwich structure. It could catalyze the hydrolysis of TPE-APP by producing TPE-DMA aggregates. As a result, the turn-on AIE fluorescence signal was assigned as "Channel I" for accurate virus detection with ultrahigh sensitivity. Meanwhile, the hydrolysis of TPE-APP could simultaneously reduce Ag^+ to form a silver nanoshell around gold nanoparticles, with a pronounced plasmonic color change, enabling the convenient naked-eye based preliminary-screening of virus (Channel II). EV71 virions can be specifically assayed with a LOD down to 1.4 copies/μL. 24 real clinical samples were diagnosed with 100% accuracy. Just through changing the recognition antibodies, H7N9 virus and Zika virus were also specifically detected. Comparing to the PCR analysis, this method did not need expensive instrument and held great potential in the wide point-of-care (POC) application.

Influenza is another type of common existing infectious diseases to both human and animal in the world. As the infection of influenza viruses to human cells depends on the binding of the trimeric hemagglutinin (HA) molecules on the virus membrane with the sialyl sugar chain receptors on the host cell membranes, the detection of influenza viruses can be realized via recognizing the HA molecules. Hatanaka's group synthesized a fluorescence oligosaccharide probes, α2,6SL-TPE, based on conjugation of 6'-sialyllactosyl moiety with TPE derivative via click reaction[121]. As the sialic acids in the α2,6SL-TPE could target the HA molecules that densely expressed (about 1000 molecules/virus) on the surface of human influenza virus, the AIE fluorescence of the α2,6SL-TPE was turned on after their binding, resulting a specific and sensitive detection of the viruses with a LOD down to 10^5 pfu/100 μL (plaque forming unit/100 μL).

Perspective

Pathogenic detection

An ideal detection method needs to be easy to use (no requirement of expensive instrument or complicated operation), rapid (capable of delivering results within a short time), reliable (high sensitivity and specificity) and cost effective (simple and can be employed in any global setting). POC testing, which could meet all these standards, is competitive for pathogenic detection in nonlaboratory settings[122]. Especially with the increasing prevalence of MDR and the need of more tailored therapeutic interventions, efficient POC tests for bacterial infections will help to identify the effective antibiotic for a patient's infection

and rule out antibiotic abuse, thus reducing the produce of pathogenic resistance. In the popular POC based assays, chromogenic medias are usually involved and provide colorimetric or fluorescent signals after responding to the target pathogens, with reduced workload and enhanced detection performance[123, 124]. As a superior choice for luminophore, AIEgen integrated POC system would be prospective in the detection of pathogen.

The capability of discrimination of pathogen from mammalian cells is another requirement for the clinical application of antimicrobial reagents, which need high selectivity towards pathogen and low toxicity to mammalian cells. Unfortunately, as the ancestor of mitochondria according to the endosymbiosis hypothesis, pathogens, such as bacteria, exhibit similar electrophysiological behavior to the inner mitochondrial membrane of mammalian cells[125]. In addition, bacteria, fungi and mammalian cells shared similar negative charges within their cell membranes, as well as the similar active chemical groups in their contained macromolecules, such as phosphate, amino and carboxylate groups, etc. With the rapid advancement in antibodies, especially monoclonal antibodies (mAbs) that could specifically recognize disease microbe, it is hopeful to endow the fluorescent AIEgen with specific targeting property after conjugation with mAbs. The differences in terms of subtypes and structures in their cellular molecules would also provide guidelines for tailored design and screening of AIEgens with high targeting competence to various disease pathogens.

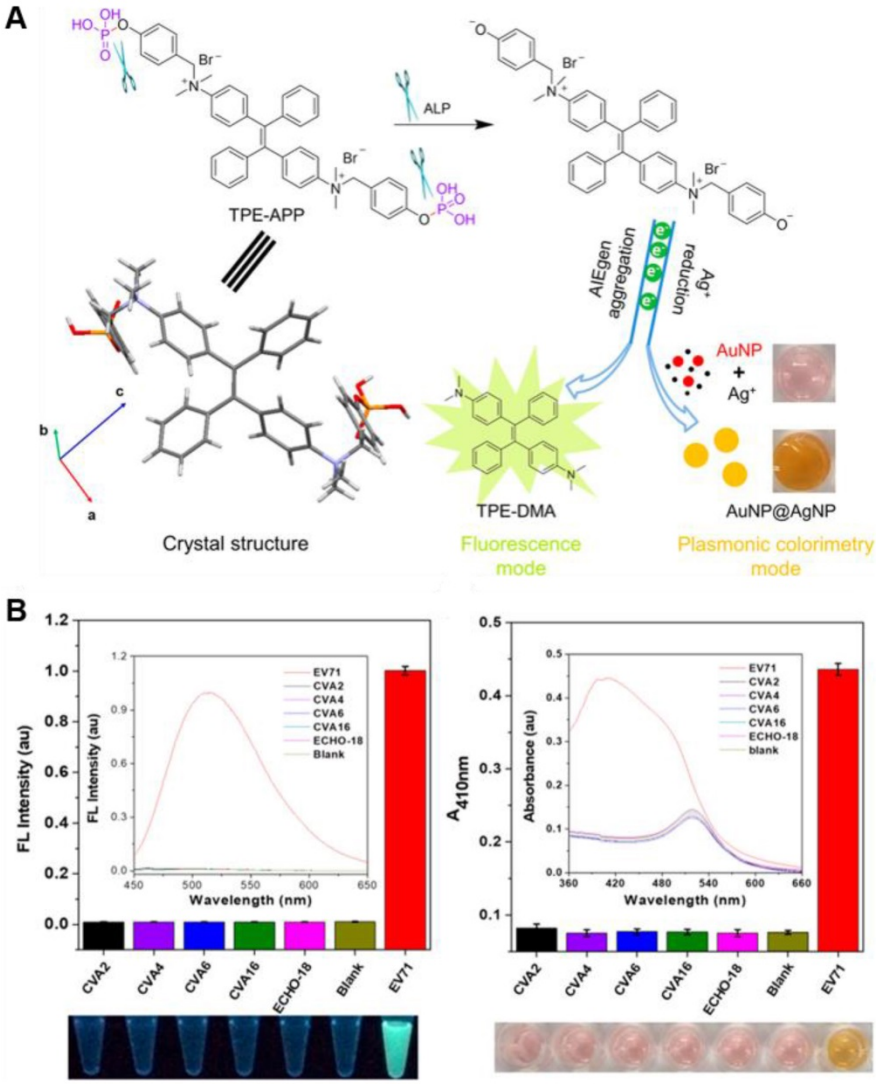

Figure 15. (A) Reaction route and single crystal structure of the multifunctional TPE-APP. It can be hydrolyzed with forming insoluble TPE-DMA aggregates and a reactive species. The resulting TPE-DMA aggregate acts as a fluorescence signal. And the redox species could generate a silver shell on the surface of AuNP, leading to a pronounced color change. **(B)** Specificity test of the dual-modality immunoassay for EV71 virion detection. Left: fluorescence intensity of various kinds of viruses, with fluorescence spectra and a photograph under UV lamp in the inset and underneath, respectively. Right: absorbance of various kinds of viruses, with absorption spectra and photograph under ambient light in the inset and underneath, respectively. Reproduced with permission from [120], copyright 2018 American Chemical Society.

Meanwhile, as increasing infections happened intra our bodies and the lack of specific biomarkers in the body fluid (i.e., blood, urine or saliva), the in situ and noninvasive detection of pathogenic infection *in vivo*, is another difficult task. Up to now, rapid and effective *in vivo* bacterial detections and treatments have hardly been realized due to lack of well-developed tools and methods. In the past years, a library of AIEgens with emission wavelength extending to NIR region have been reported with successful applications in bioimaging *in vivo* [126]. Beyond the sensitive fluorescence signal, successful attempts in construction of multimodal sensing platform by integrating two or more detection modes (e.g., PA, CT and MRI imaging with deep-penetration depth) with AIEgens [127-129], which could endow extra advantages such as overcoming the limitation associated with each modality, cross-validation, and maximizing their synergistic effects, were also reported one by one. It is believable that in situ imaging of pathogenic infection *in vivo* would be realized with promising AIE-based imaging system with capability of deep penetration-depth and multimodality function.

Pathogenic therapy

As the evolution of biomedical technologies, alternative approaches to address bacterial infections are springing up like mushrooms. Several promising strategies, such as phage-mediated therapy, microbiome renovation, host modulation and immunotherapeutics are highlighted below, and their possible combinations with AIE systems are also under consideration.

Phages are viruses that can infect bacteria and cause the lysis and death of the bacteria, through injecting their DNA or RNA, and using the host enzymes and cofactors to replicate[130]. They were being used as antimicrobials even before penicillin was discovered. As their specificity towards target bacteria, there is no harmful impact on mammalian cells. However, one phage typically targets only a limited number of bacterial strains, which means multiple different phages are needed to treat one species of infection. The next challenge is how to deliver the phage to the site of action since phage does not have favorable *pK* property[131]. It is promising to integrate phage with PDI-active AIE systems, for synergizing the phage's specificity and PDI's wide-spectrum antimicrobial effect. What's more, as spontaneous nanoaggregates or self-assembled supramolecular nanostructures with excellent stability and biocompatibility, AIE-based systems would act as perfect nanocarriers for targeting delivery of phage into the infection site.

Meanwhile, it has become well accepted that the human microbiome (e.g., microorganism living in gut and stomach), plays a significant role on the health and stability of the host[132, 133]. Certain probiotics are able to combat pathogens through the secretion of antimicrobial substances and organic acids or through competing for resources and space[134]. However, the overuse of broad-spectrum antibiotics could eliminate large portions of the probiotic and cause opportunistic pathogenic bacteria to establish in some circumstances. As an efficient tool in antibiotics screening and susceptibility evaluation, AIE-based system might contribute to restore microbiome and provide a rich source of therapies for a wide range of pathogenic infections.

As more and more host immune and inflammation systems are being discovered, increasing researches are aiming to improve the host response to fight pathogens beyond the exploration of antimicrobial reagents[135]. Although vaccination programs are prevalent in virus prevention, immunotherapeutics are relatively unexplored for bacterial and fungal infections, since no targets are validated for bacterial or fungal infection. Functional nanoparticles or supramolecular nanostructures, which possess the similar diameters and interfaces as the antigen proteins, have been tested as immunotherapeutic agents to treat various diseases, especially in cancer treatment[136]. AIE-based functional nanoaggregates and self-assembly supramolecular nanostructures, would therefore, offer great potentials for host modulation and immunotherapeutic treatment of pathogenic infection.

Conclusion

In conclusion, we discussed various types of AIE-based supramolecular systems that had been developed for pathogen detection, differentiation and killing. They are derived from amphiphilic molecules with noncovalent assembly, reactive/responsive molecules with covalent linking, multifunctional structures through conjugation with functional peptides, polymers, host-gust materials or nano-frameworks, nanosized aggregates, integrated molecules or structures with multimodality imaging or killing properties and so on. Their unique turn-on fluorescent properties with large Stokes' shift, robust luminosity, strong photobleaching resistance, no random blinking and tunability in emission color even to NIR range, make them superior choices for multiple pathogenic identification, pathogenicity/ virulence evaluation, antimicrobial drugs screening and long-term infection monitoring ranging from *in vitro* to *in vivo*. On the other hand, the flexibility in

molecular designing and supramolecular regulation of the AIE-based systems would be endowed with desired dark-toxic and PDI moieties on their structures or interfaces, which could perform excellently in pathogenic binding and killing in their aggregated states. We believe that a coordinated effort in research and development of new agents by taking advantages of the unique AIE-based supramolecular systems would provide great potentials for the early prevention of pathogenic infection and benefit the public healthcare.

Abbreviations

G^+: Gram-positive; G^-: Gram-negative; AIE: aggregation-induced emission; AIEgens: luminogens with aggregation-induced emission; AIEE: aggregation-induced enhanced emission; PDI: photodynamic inactivation; ELISA: enzyme-linked immunosorbent assay; PCR: polymerase chain reaction; TPE: tetraphenylethene; TriPE: triphenylethylene; TPA: triphenylamine; TPIM: tetraphenyl imidazole; IQ: diphenyl isoquinolinium; TPP: tetraphenylpyrazine; RIM: restriction of intramolecular motion; ROS: reactive oxygen species; MDR: multiple drug resistance; F-array: fluorescent array; ICT: intramolecular charge transfer; ESIPT: excited-state intramolecular proton transfer; HBT: 2-(2-Hydroxyphenyl) benzothiazole; CMC: critical micelle concentration; CFU: colony-forming unit; PFU: plaque forming unit; LOD: limit of detection; NIR: near infrared; DPP: diketopyrrolopyrrole; TPE-2BA: TPE with two phenylboronic acid; TriPE-3BA: (4-(2,2-bis(4-boronophenyl)vinyl)phenyl)-boronic acid; TPE-4BA: ethene-1,1,2,2-tetrayltetrakis-(benzene-4,1-diyl)tetraboronic acid; Glc-bis: bisacrylamide; Glc-acryl: monoacry-lamide; GO: graphene oxide; TPE4S: tetraphenylethene luminogen; BV: Bacterial vaginosis; ZnDPA: zinc (II)-dipicolylamine; AIE-ZnDPA: AIE-Zinc (II)-dipicolylamine; AIP: aggregation induced phosphorescence; MIC: minimum inhibitory concentration; AMP: antimicrobial peptides; Van: vancomycin; PIC: polyion complex; PEO-*b*-PQDMA: poly(ethylene oxide)-*b*-quaternized poly(2-(dimethylamino)ethyl methacrylate); DBPE-DBO: 1,2-diphenyl-1,2-bis(4-(pyridin-4-yl)phenyl)ethane-1, 8-dibromooctane; PSMA: polystyrene-*co*-maleic anhydride; ALP: alkaline phosphatase; TPFL: two-photon fluorescent; PBS: buffered saline; PNDs: pure nanodrugs; FONs: fluorescent organic nanoparticles; MOFs: metal-organic frameworks; TPEDB: 4,4′-(1,2-diphenylethene-1,2-diyl)bis(1,4-phenylene)diboronic acid; PEI: polyethyleneimine; CD: cyclodextrin; MSNs: mesoporous silica nanoparticles; AMO: amoxicillin; PGEDA: polyglycerol methacrylate; CB[7]: cucurbit[7]uril; KB-1: 4-((pyren-1-ylmethylene) amino)phenol; PET: photoinduced electron transfer; M1-DPAN: 2-(((diphenylmethylene)hydrazono) methyl) naphthalene; LTA: lipoteichoic acid; LPS: lipopolysaccharides; MRI: magnetic resonance imaging; CLSM: confocal laser scanning microscopy; POC: point-of-care; mAbs: monoclonal antibodies; PI: propidium iodide.

Acknowledgements

The authors acknowledge funding to B.Z.T. from the Research Grants Council of Hong Kong (N_HKUST604/14 and C6009-17G), the Innovation and Technology Commission (ITC-CNERC14SC01), and the National Key Research and Development program of China (2018YFE0190200). B.Z.T. is also grateful for the support from the Science and Technology Plan of Shenzhen (JCYJ20160229 205601482). And funding to L.-H. X. from the National Science Foundation of China (21705111).

Competing Interests

The authors have declared that no competing interest exists.

References

1. Casadevall A, Pirofski L-a. Microbiology: ditch the term pathogen. Nature. 2014; 516: 165-6.
2. Anderson RM, May RM. Population biology of infectious diseases: Part I. Nature. 1979; 280: 361-7.
3. Wolfe ND, Dunavan CP, Diamond J. Origins of major human infectious diseases. Nature. 2007; 447: 279-83.
4. Schlecht LM, Peters BM, Krom BP, Freiberg JA, Hänsch GM, Filler SG, et al. Systemic Staphylococcus aureus infection mediated by Candida albicans hyphal invasion of mucosal tissue. Microbiology. 2015; 161: 168-81.
5. Duerkop BA, Hooper LV. Resident viruses and their interactions with the immune system. Nat Immunol. 2013; 14: 654-9.
6. Romani L. Immunity to fungal infections. Nat Rev Immunol. 2011; 11: 275-88.
7. Ray PC, Khan SA, Singh AK, Senapati D, Fan Z. Nanomaterials for targeted detection and photothermal killing of bacteria. Chem Soc Rev. 2012; 41: 3193-209.
8. Li Z, Askim JR, Suslick KS. The optoelectronic nose: colorimetric and fluorometric sensor arrays. Chem Rev. 2018; 119: 231-92.
9. Yu X, Xia Y, Tang Y, Zhang WL, Yeh YT, Lu H, et al. A nanostructured microfluidic immunoassay platform for highly sensitive infectious pathogen detection. Small. 2017; 13: 1700425.
10. Wu Z, Hu J, Zeng T, Zhang Z-L, Chen J, Wong G, et al. Ultrasensitive ebola virus detection based on electroluminescent nanospheres and immunomagnetic separation. Anal Chem. 2017; 89: 2039-48.
11. Brussaard CP, Marie D, Bratbak G. Flow cytometric detection of viruses. J Virol Methods 2000; 85: 175-82.
12. Steininger C, Kundi M, Aberle SW, Aberle JH, Popow-Kraupp T. Effectiveness of reverse transcription-PCR, virus isolation, and enzyme-linked immunosorbent assay for diagnosis of influenza A virus infection in different age groups. J Clin Microbiol. 2002; 40: 2051-6.
13. Kohanski MA, Dwyer DJ, Collins JJ. How antibiotics kill bacteria: from targets to networks. Nat Rev Microbiol. 2010; 8: 423-35.
14. Downard KM. Proteotyping for the rapid identification of influenza virus and other biopathogens. Chem Soc Rev. 2013; 42: 8584-95.
15. Váradi L, Luo JL, Hibbs DE, Perry JD, Anderson RJ, Orenga S, et al. Methods for the detection and identification of pathogenic bacteria: past, present, and future. Chem Soc Rev. 2017; 46: 4818-32.
16. Ghannoum MA, Rice LB. Antifungal agents: mode of action, mechanisms of resistance, and correlation of these mechanisms with bacterial resistance. Clin Microbiol Rev. 1999; 12: 501-17.
17. Baker M. Whole-animal imaging: the whole picture. Nature. 2010; 463: 977-80.
18. Kobayashi H, Ogawa M, Alford R, Choyke PL, Urano Y. New strategies for fluorescent probe design in medical diagnostic imaging. Chem Rev. 2010; 110: 2620-40.

19. Mei J, Hong Y, Lam JW, Qin A, Tang Y, Tang BZ. Aggregation-induced emission: the whole is more brilliant than the parts. Adv Mater. 2014; 26: 5429-79.
20. He X, Zeng T, Li Z, Wang G, Ma N. Catalytic molecular imaging of microRNA in living cells by DNA-programmed nanoparticle disassembly. Angew Chem Int Ed. 2016; 55: 3073-6.
21. Wei W, He X, Ma N. DNA-templated assembly of a heterobivalent quantum dot nanoprobe for extra- and intracellular dual-targeting and imaging of live cancer cells. Angew Chem Int Ed. 2014; 53: 5573-7.
22. He X, Li Z, Chen M, Ma N. DNA-programmed dynamic assembly of quantum dots for molecular computation. Angew Chem Int Ed. 2014; 53: 14447-50.
23. He X, Ma N. An overview of recent advances in quantum dots for biomedical applications. Colloid Surf B Biointerfaces. 2014; 124: 118-31.
24. He X, Ma N. A general strategy for label-free sensitive DNA detection based on quantum dot doping. Anal Chem. 2014; 86: 3676-81.
25. He X, Gao L, Ma N. One-step instant synthesis of protein-conjugated quantum dots at room temperature. Sci Rep. 2013; 3: 2825.
26. He X, Ma N. Biomimetic synthesis of fluorogenic quantum dots for ultrasensitive label-free detection of protease activities. Small. 2013; 9: 2527-31.
27. Zeng T, Zhang T, Wei W, Li Z, Wu D, Wang L, et al. Compact, programmable, and stable biofunctionalized upconversion nanoparticles prepared through peptide-mediated phase transfer for high-sensitive protease sensing and *in vivo* apoptosis imaging. ACS Appl Mater Interfaces. 2015; 7: 11849-56.
28. Li Z, He X, Luo X, Wang L, Ma N. DNA-programmed quantum dot polymerization for ultrasensitive molecular imaging of cancer cells. Anal Chem. 2016; 88: 9355-8.
29. Luo X, Li Z, Wang G, He X, Shen X, Sun Q, et al. MicroRNA-catalyzed cancer therapeutics based on DNA-programmed nanoparticle complex. ACS Appl Mater Interfaces. 2017; 9: 33624-31.
30. Wu D, Song G, Li Z, Zhang T, Wei W, Chen M, et al. A two-dimensional molecular beacon for mRNA-activated intelligent cancer theranostics. Chem Sci. 2015; 6: 3839-44.
31. Li Z, Wang G, Shen Y, Guo N, Ma N. DNA-templated magnetic nanoparticle-quantum dot polymers for ultrasensitive capture and detection of circulating tumor cells. Adv Funct Mater. 2018; 28: 1707152.
32. Ma N, Sargent EH, Kelley SO. One-step DNA-programmed growth of luminescent and biofunctionalized nanocrystals. Nat Nanotechnol. 2009; 4: 121-5.
33. Kwok RTK, Leung CWT, Lam JWY, Tang BZ. Biosensing by luminogens with aggregation-induced emission characteristics. Chem Soc Rev. 2015; 44: 4228-38.
34. Hong Y, Lam JWY, Tang BZ. Aggregation-induced emission. Chem Soc Rev. 2011; 40: 5361-88.
35. Luo J, Xie Z, Lam JW, Cheng L, Chen H, Qiu C, et al. Aggregation-induced emission of 1-methyl-1, 2, 3, 4, 5-pentaphenylsilole. Chem Commun. 2001: 1740-1.
36. Tong H, Hong Y, Dong Y, Häußler M, Lam JWY, Li Z, et al. Fluorescent "light-up" bioprobes based on tetraphenylethylene derivatives with aggregation-induced emission characteristics. Chem Commun. 2006: 3705-7.
37. Kong TT, Zhao Z, Li Y, Wu F, Jin T, Tang BZ. Detecting live bacteria instantly utilizing AIE strategies. J Mater Chem B. 2018; 6: 5986-91.
38. Wang D, Su H, Kwok RTK, Hu X, Zou H, Luo Q, et al. Rational design of a water-soluble NIR AIEgen, and its application in ultrafast wash-free cellular imaging and photodynamic cancer cell ablation. Chem Sci. 2018; 9: 3685-93.
39. Gao T, Cao X, Dong J, Liu Y, Lv W, Li C, et al. A novel water soluble multifunctional fluorescent probe for highly sensitive and ultrafast detection of anionic surfactants and wash free imaging of Gram-positive bacteria strains. Dyes and Pigments. 2017; 143: 436-43.
40. Gui C, Zhao E, Kwok RTK, Leung ACS, Lam JWY, Jiang M, et al. AIE-active theranostic system: selective staining and killing of cancer cells. Chem Sci. 2017; 8: 1822-30.
41. Chen M, Li L, Nie H, Tong J, Yan L, Xu B, et al. Tetraphenylpyrazine-based AIEgens: facile preparation and tunable light emission. Chem Sci. 2015; 6: 1932-7.
42. Feng X, Qi C, Feng H-T, Zhao Z, Sung HHY, Williams ID, et al. Dual fluorescence of tetraphenylethylene-substituted pyrenes with aggregation-induced emission characteristics for white-light emission. Chem Sci. 2018; 9: 5679-87.
43. Zhu C, Kwok RTK, Lam JWY, Tang BZ. Aggregation-induced emission: a trailblazing journey to the field of biomedicine. ACS Appl Bio Mater. 2018; 1: 1768-86.
44. Mei J, Leung NL, Kwok RT, Lam JW, Tang BZ. Aggregation-induced emission: together we shine, united we soar! Chem Rev. 2015; 115: 11718-940.
45. Ni X, Zhang X, Duan X, Zheng H-L, Xue X-S, Ding D. Near-infrared afterglow luminescent aggregation-induced emission dots with ultrahigh tumor-to-liver signal ratio for promoted image-guided cancer surgery. Nano Lett. 2018; 19: 318-30.
46. Gao H, Zhang X, Chen C, Li K, Ding D. Unity makes strength: how aggregation-induced emission luminogens advance the biomedical field. Adv Biosys. 2018; 2: 1800074.
47. Qi J, Chen C, Ding D, Tang BZ. Aggregation-induced emission luminogens: union is strength, gathering illuminates healthcare. Adv Healthcare Mater. 2018; 7: 1800477.
48. Fu W, Yan C, Guo Z, Zhang J, Zhang H, Tian H, et al. Rational design of near-infrared AIE-active probes: in situ mapping of amyloid-β plaques with ultra-sensitivity and high-fidelity. J Am Chem Soc. 2019; 141: 3171-7.
49. Zhang J, Wang Q, Guo Z, Zhang S, Yan C, Tian H, et al. High-fidelity trapping of spatial–temporal mitochondria with rational design of aggregation-induced emission probes. Adv Funct Mater. 2019; 29: 1808153.
50. Shao A, Xie Y, Zhu S, Guo Z, Zhu S, Guo J, et al. Far-red and near-IR AIE-active fluorescent organic nanoprobes with enhanced tumor-targeting efficacy: shape-specific effects. Angew Chem Int Ed. 2015; 54: 7275-80.
51. Zhao Z, Chen C, Wu W, Wang F, Du L, Zhang X, et al. Highly efficient photothermal nanoagent achieved by harvesting energy via excited-state intramolecular motion within nanoparticles. Nat Commun. 2019; 10: 768.
52. Xie S, Wong AY, Kwok RT, Li Y, Su H, Lam JW, et al. Fluorogenic Ag^{+}–tetrazolate aggregation enables efficient fluorescent biological silver staining. Angew Chem Int Ed. 2018; 57: 5750-3.
53. Zhao Z, Su H, Zhang P, Cai Y, Kwok RT, Chen Y, et al. Polyyne bridged AIE luminogens with red emission: design, synthesis, properties and applications. J Mater Chem B. 2017; 5: 1650-7.
54. Feng X, Li Y, He X, Liu H, Zhao Z, Kwok RT, et al. A substitution-dependent light-up fluorescence probe for selectively detecting Fe^{3+} Ions and its cell imaging application. Adv Funct Mater. 2018; 28: 1802833.
55. Niu G, Zhang R, Kwong JP, Lam JW, Chen C, Wang J, et al. Specific two-photon imaging of live cellular and deep-tissue lipid droplets by lipophilic AIEgens at ultralow concentration. Chem Mater. 2018; 30: 4778-87.
56. Li K, Feng Q, Niu G, Zhang W, Li Y, Kang M, et al. Benzothiazole-based AIEgen with tunable excited-state intramolecular proton transfer and restricted intramolecular rotation processes for highly sensitive physiological pH sensing. ACS Sens. 2018; 3: 920-8.
57. Dang D, Liu H, Wang J, Chen M, Liu Y, Sung HH-Y, et al. Highly emissive AIEgens with multiple functions: facile synthesis, chromism, specific lipid droplet imaging, apoptosis monitoring, and *in vivo* imaging. Chem Mater. 2018; 30: 7892-901.
58. He X, Yin F, Wang D, Xiong L-H, Kwok RTK, Gao PF, et al. AIE featured inorganic–organic core@shell nanoparticle for high-efficiency siRNA delivery and real-time monitoring. Nano Lett. 2019; 19: 2272–9.
59. Gao M, Tang BZ. Fluorescent sensors based on aggregation-induced emission: recent advances and perspectives. ACS Sens. 2017; 2: 1382-99.
60. Wang D, Lee MMS, Xu W, Kwok RTK, Lam JWY, Tang BZ. Theranostics based on AIEgens. Theranostics. 2018; 8: 4925-56.
61. Wang D, Lee MM, Shan G, Kwok RT, Lam JW, Su H, et al. Highly efficient photosensitizers with far-red/near-infrared aggregation-induced emission for *in vitro* and *in vivo* cancer theranostics. Adv Mater. 2018; 30: 1802105.
62. Zheng Z, Zhang T, Liu H, Chen Y, Kwok RT, Ma C, et al. Bright near-infrared aggregation-induced emission luminogens with strong two-photon absorption, excellent organelle specificity, and efficient photodynamic therapy potential. ACS Nano. 2018; 12: 8145-59.
63. Hu F, Xu S, Liu B. Photosensitizers with aggregation-induced emission: materials and biomedical applications. Adv Mater. 2018; 30: 1801350.
64. Bennett L, Ghiggino K, Henderson R. Singlet oxygen formation in monomeric and aggregated porphyrin c. J Photochem Photobiol B. 1989; 3: 81-9.
65. Liu G-j, Tian S-n, Li C-y, Xing G-w, Zhou L. Aggregation-induced-emission materials with different electric charges as an artificial tongue: design, construction, and assembly with various pathogenic bacteria for effective bacterial imaging and discrimination. ACS Appl Mater Interfaces. 2017; 9: 28331-8.
66. Jiang M, Gu X, Kwok RTK, Li Y, Sung HHY, Zheng X, et al. Multifunctional AIEgens: ready synthesis, tunable emission, mechanochromism, mitochondrial, and bacterial imaging. Adv Funct Mater. 2018; 28: 1704589.
67. Gao M, Wang L, Chen J, Li S, Lu G, Wang L, et al. Aggregation-induced emission active probe for light-up detection of anionic surfactants and wash-free bacterial imaging. Chem Eur J. 2016; 22: 5107-12.
68. Hamblin MR, Hasan T. Photodynamic therapy: a new antimicrobial approach to infectious disease? Photoch Photobiol Sci. 2004; 3: 436-50.
69. Jiang G, Wang J, Yang Y, Zhang G, Liu Y, Lin H, et al. Fluorescent turn-on sensing of bacterial lipopolysaccharide in artificial urine sample with sensitivity down to nanomolar by tetraphenylethylene based aggregation induced emission molecule. Biosens Bioelectron. 2016; 85: 62-7.
70. Zhao E, Chen Y, Chen S, Deng H, Gui C, Leung CWT, et al. A luminogen with aggregation-induced emission characteristics for wash-free bacterial imaging, high-throughput antibiotics screening and bacterial susceptibility evaluation. Adv Mater. 2015; 27: 4931-7.
71. Hu R, Zhou F, Zhou T, Shen J, Wang Z, Zhao Z, et al. Specific discrimination of gram-positive bacteria and direct visualization of its infection towards mammalian cells by a DPAN-based AIEgen. Biomaterials. 2018; 187: 47-54.
72. Almeida A, Faustino MA, Tomé JP. Photodynamic inactivation of bacteria: finding the effective targets. Future Med Chem. 2015; 7: 1221-4.
73. Zhao E, Chen Y, Wang H, Chen S, Lam JWY, Leung CWT, et al. Light-enhanced bacterial killing and wash-free imaging based on AIE fluorogen. ACS Appl Mater Interfaces. 2015; 7: 7180-8.
74. You X, Ma H, Wang Y, Zhang G, Peng Q, Liu L, et al. Pyridinium-substituted tetraphenylethylene entailing alkyne moiety: enhancement of photosensitizing efficiency and antimicrobial activity. Chem Asian J. 2017; 12: 1013-9.
75. Wallace BD, Wang H, Lane KT, Scott JE, Orans J, Koo JS, et al. Alleviating cancer drug toxicity by inhibiting a bacterial enzyme. Science. 2010; 330: 831-5.

76. Yu T, Guo F, Yu Y, Sun T, Ma D, Han J, et al. Fusobacterium nucleatum promotes chemoresistance to colorectal cancer by modulating autophagy. Cell. 2017; 170: 548-63.
77. Kang M, Kwok RTK, Wang J, Zhang H, Lam JWY, Li Y, et al. A multifunctional luminogen with aggregation-induced emission characteristics for selective imaging and photodynamic killing of both cancer cells and Gram-positive bacteria. J Mater Chem B. 2018; 6: 3894-903.
78. Li Y, Zhao Z, Zhang J, Kwok RTK, Xie S, Tang R, et al. A bifunctional aggregation-induced emission luminogen for monitoring and killing of multidrug-resistant bacteria. Adv Funct Mater. 2018; 28: 1804632.
79. Weintraub A. Immunology of bacterial polysaccharide antigens. Carbohyd Res. 2003; 338: 2539-47.
80. Liu Y, Deng C, Tang L, Qin A, Hu R, Sun JZ, et al. Specific detection of D-glucose by a tetraphenylethene-based fluorescent sensor. J Am Chem Soc. 2010; 133: 660-3.
81. Zhao E, Hong Y, Chen S, Leung CWT, Chan CYK, Kwok RTK, et al. Highly fluorescent and photostable probe for long-term bacterial viability assay based on aggregation-induced emission. Adv Healthcare Mater. 2014; 3: 88-96.
82. Hu X, Zhao X, He B, Zhao Z, Zheng Z, Zhang P, et al. A simple approach to bioconjugation at diverse levels: metal-free click reactions of activated alkynes with native groups of biotargets without prefunctionalization. Research. 2018; 2018: 3152870.
83. Engler AC, Wiradharma N, Ong ZY, Coady DJ, Hedrick JL, Yang Y-Y. Emerging trends in macromolecular antimicrobials to fight multi-drug-resistant infections. Nano Today. 2012; 7: 201-22.
84. Bertozzi CR, Kiessling LL. Chemical glycobiology. Science. 2001; 291: 2357-64.
85. Ajish JK, Kumar KA, Ruhela A, Subramanian M, Ballal AD, Kumar M. AIE based fluorescent self assembled glycoacrylamides for E. coli detection and cell imaging. Sensor Actuat B-Chem. 2018; 255: 1726-34.
86. Hartmann M, Lindhorst TK. The bacterial lectin FimH, a target for drug discovery–carbohydrate inhibitors of type 1 fimbriae-mediated bacterial adhesion. Eur J Org Chem. 2011;: 3583-609.
87. Hang Y, He X-P, Yang L, Hua J. Probing sugar–lectin recognitions in the near-infrared region using glyco-diketopyrrolopyrrole with aggregation-induced-emission. Biosens Bioelectron. 2015; 65: 420-6.
88. Jiang T, Tan H, Sun Y, Wang J, Hang Y, Lu N, et al. Graphene oxide-based NIR fluorescence probe with aggregation-induced emission property for lectins detection and liver cells targeting. Sensors and Actuators B: Chemical. 2018; 261: 115-26.
89. Corfield T. Bacterial sialidases—roles in pathogenicity and nutrition. Glycobiology. 1992; 2: 509-21.
90. Myziuk L, Romanowski B, Johnson SC. BVBlue test for diagnosis of bacterial vaginosis. J Clin Microbiol. 2003; 41: 1925-8.
91. Liu G-j, Wang B, Zhang Y, Xing G-w, Yang X, Wang S. A tetravalent sialic acid-coated tetraphenylethene luminogen with aggregation-induced emission characteristics: design, synthesis and application for sialidase activity assay, high-throughput screening of sialidase inhibitors and diagnosis of bacterial vaginosis. Chem Commun. 2018; 54: 10691-4.
92. Gao M, Hu Q, Feng G, Tomczak N, Liu R, Xing B, et al. A multifunctional probe with aggregation-induced emission characteristics for selective fluorescence imaging and photodynamic killing of bacteria over mammalian cells. Adv Healthcare Mater. 2015; 4: 659-63.
93. Feng G, Zhang C-J, Lu X, Liu B. Zinc(II)-tetradentate-coordinated probe with aggregation-induced emission characteristics for selective imaging and photoinactivation of bacteria. ACS Omega. 2017; 2: 546-53.
94. Jain N, Alam P, Laskar IR, Panwar J. 'Aggregation induced phosphorescence' active iridium(iii) complexes for integrated sensing and inhibition of bacterial growth in aqueous solution. RSC Adv. 2015; 5: 61983-8.
95. Fjell CD, Hiss JA, Hancock RE, Schneider G. Designing antimicrobial peptides: form follows function. Nat Rev Drug Discov. 2012; 11: 37-51.
96. Hancock RE, Scott MG. The role of antimicrobial peptides in animal defenses. Proc Natl Acad Sci USA. 2000; 97: 8856-61.
97. Yu G, Baeder DY, Regoes RR, Rolff J. The more the better? Combination effects of antimicrobial peptides. Antimicrob Agents CH. 2016; 60: 1717-24.
98. Li NN, Li JZ, Liu P, Pranantyo D, Luo L, Chen JC, et al. An antimicrobial peptide with an aggregation-induced emission (AIE) luminogen for studying bacterial membrane interactions and antibacterial actions. Chem Commun. 2017; 53: 3315-8.
99. Chen J, Gao M, Wang L, Li S, He J, Qin A, et al. Aggregation-induced emission probe for study of the bactericidal mechanism of antimicrobial peptides. ACS Appl Mater Interfaces. 2018; 10: 11436-42.
100. Feng G, Yuan Y, Fang H, Zhang R, Xing B, Zhang G, et al. A light-up probe with aggregation-induced emission characteristics (AIE) for selective imaging, naked-eye detection and photodynamic killing of gram-positive bacteria. Chem Commun. 2015; 51: 12490-3.
101. Zhang R, Cai X, Feng G, Liu B. Real-time naked-eye multiplex detection of toxins and bacteria using AIEgens with the assistance of graphene oxide. Faraday Discussions. 2017; 196: 363-75.
102. Li Y, Hu X, Tian S, Li Y, Zhang G, Zhang G, et al. Polyion complex micellar nanoparticles for integrated fluorometric detection and bacteria inhibition in aqueous media. Biomaterials. 2014; 35: 1618-26.
103. Li Y, Yu H, Qian Y, Hu J, Liu S. Amphiphilic star copolymer-based bimodal fluorogenic/magnetic resonance probes for concomitant bacteria detection and inhibition. Adv Mater. 2014; 26: 6734-41.
104. Zhao J, Dong Z, Cui H, Jin H, Wang C. Nanoengineered peptide-grafted hyperbranched polymers for killing of bacteria monitored in real time via intrinsic aggregation-induced emission. ACS Appl Mater Interfaces. 2018; 10: 42058-67.
105. Ma H, Ma Y, Lei L, Yin W, Yang Y, Wang T, et al. Light-enhanced bacterial killing and less toxic cell imaging: multicationic aggregation-induced emission matters. ACS Sustain Chem Eng. 2018; 6: 15064-71.
106. Zhao L, Chen Y, Yuan J, Chen M, Zhang H, Li X. Electrospun fibrous mats with conjugated tetraphenylethylene and mannose for sensitive turn-On fluorescent sensing of escherichia coli. ACS Appl Mater Interfaces. 2015; 7: 5177-86.
107. Kang EB, Mazrad ZAI, Robby AI, In I, Park SY. Alkaline phosphatase-responsive fluorescent polymer probe coated surface for colorimetric bacteria detection. Eur Polym J. 2018; 105: 217-25.
108. Yang X, Wang N, Zhang L, Dai L, Shao H, Jiang X. Organic nanostructure-based probes for two-photon imaging of mitochondria and microbes with emission between 430 nm and 640 nm. Nanoscale. 2017; 9: 4770-6.
109. Xie S, Manuguri S, Proietti G, Romson J, Fu Y, Inge AK, et al. Design and synthesis of theranostic antibiotic nanodrugs that display enhanced antibacterial activity and luminescence. Proc Natl Acad Sci USA. 2017; 114: 8464-9.
110. Gao T, Zeng H, Xu H, Gao F, Li W, Zhang S, et al. Novel self-assembled organic nanoprobe for molecular imaging and treatment of gram-positive bacterial infection. Theranostics. 2018; 8: 1911-22.
111. Mao D, Hu F, Kenry, Ji S, Wu W, Ding D, et al. Metal–organic-framework-assisted *in vivo* bacterial metabolic labeling and precise antibacterial therapy. Adv Mater. 2018; 30: 1706831.
112. Wu Y, Chen Q, Li Q, Lu H, Wu X, Ma J, et al. Daylight-stimulated antibacterial activity for sustainable bacterial detection and inhibition. J Mater Chem B. 2016; 4: 6350-7.
113. Li Q, Wu Y, Lu H, Wu X, Chen S, Song N, et al. Construction of supramolecular nanoassembly for responsive bacterial elimination and effective bacterial detection. ACS Appl Mater Interfaces. 2017; 9: 10180-9.
114. Kathiravan A, Sundaravel K, Jaccob M, Dhinagaran G, Rameshkumar A, Arul Ananth D, et al. Pyrene schiff base: photophysics, aggregation Induced emission, and antimicrobial properties. J Phys Chem B. 2014; 118: 13573-81.
115. Maurya N, Singh AK. Indirect approach for CN− detection via Cu2+ induced turn-off sensor: Using novel AIEE fluorophore with logic gate and antimicrobial application. Dyes and Pigments. 2017; 147: 484-90.
116. Chen W, Li Q, Zheng W, Hu F, Zhang G, Wang Z, et al. Identification of bacteria in water by a fluorescent array. Angew Chem Int Ed. 2014; 53: 13734-9.
117. Zhou C, Xu W, Zhang P, Jiang M, Chen Y, Kwok RTK, et al. Engineering sensor arrays using aggregation-induced emission luminogens for pathogen identification. Adv Funct Mater. 2019; 29: 1805986.
118. Klein G, Schanstra JP, Hoffmann J, Mischak H, Siwy J, Zimmermann K. Proteomics as a quality control tool of pharmaceutical probiotic bacterial lysate products. PloS one. 2013; 8: e66682.
119. Shen J, Hu R, Zhou T, Wang Z, Zhang Y, Li S, et al. Fluorescent sensor array for highly efficient microbial lysate identification through competitive interactions. ACS Sensors. 2018; 3: 2218-22.
120. Xiong L-H, He X, Zhao Z, Kwok RTK, Xiong Y, Gao PF, et al. Ultrasensitive virion immunoassay platform with dual-modality based on a multifunctional aggregation-induced emission luminogen. ACS Nano. 2018; 12: 9549-57.
121. Kato T, Kawaguchi A, Nagata K, Hatanaka K. Development of tetraphenylethylene-based fluorescent oligosaccharide probes for detection of influenza virus. Biochem Bioph Res Commun. 2010; 394: 200-4.
122. Granger JH, Schlotter NE, Crawford AC, Porter MD. Prospects for point-of-care pathogen diagnostics using surface-enhanced Raman scattering (SERS). Chem Soc Rev. 2016; 45: 3865-82.
123. Xiong L-H, He X, Xia J, Ma H, Yang F, Zhang Q, et al. Highly sensitive naked-eye assay for enterovirus 71 detection based on catalytic nanoparticle aggregation and immunomagnetic amplification. ACS Appl Mater Interfaces. 2017; 9: 14691-9.
124. Xiong L-H, Cui R, Zhang Z-L, Yu X, Xie Z, Shi Y-B, et al. Uniform fluorescent nanobioprobes for pathogen detection. ACS Nano. 2014; 8: 5116-24.
125. Walden WE. From bacteria to mitochondria: aconitase yields surprises. Proc Natl Acad Sci USA. 2002; 99: 4138-40.
126. Qian J, Tang BZ. AIE luminogens for bioimaging and theranostics: from organelles to animals. Chem. 2017; 3: 56-91.
127. He X, Zhao Z, Xiong L-H, Gao PF, Peng C, Li RS, et al. Redox-active AIEgen derived plasmonic and fluorescent core@shell nanoparticles for multimodality bioimaging. J Am Chem Soc. 2018; 140: 6904-11.
128. Mahtab F, Yu Y, Lam JW, Liu J, Zhang B, Lu P, et al. Fabrication of silica nanoparticles with both efficient fluorescence and strong magnetization and exploration of their biological applications. Adv Funct Mater. 2011; 21: 1733-40.
129. Qi J, Chen C, Zhang X, Hu X, Ji S, Kwok RT, et al. Light-driven transformable optical agent with adaptive functions for boosting cancer surgery outcomes. Nat Commun. 2018; 9: 1848.
130. Levin BR, Bull JJ. Population and evolutionary dynamics of phage therapy. Nat Rev Microbiol. 2004; 2: 166-73.

131. Nobrega FL, Vlot M, de Jonge PA, Dreesens LL, Beaumont HJE, Lavigne R, et al. Targeting mechanisms of tailed bacteriophages. Nat Rev Microbiol. 2018; 16: 760-73.
132. Thaiss CA, Zmora N, Levy M, Elinav E. The microbiome and innate immunity. Nature. 2016; 535: 65-74.
133. Kau AL, Ahern PP, Griffin NW, Goodman AL, Gordon JI. Human nutrition, the gut microbiome and the immune system. Nature. 2011; 474: 327-36.
134. Li Z, Behrens AM, Ginat N, Tzeng SY, Lu X, Sivan S, et al. Biofilm-inspired encapsulation of probiotics for the treatment of complex infections. Adv Mater. 2018: 1803925.
135. Pirofski L-a, Casadevall A. Immunomodulators as an antimicrobial tool. Curr Opin Microbiol. 2006; 9: 489-95.
136. Irvine DJ, Hanson MC, Rakhra K, Tokatlian T. Synthetic nanoparticles for vaccines and immunotherapy. Chem Rev. 2015; 115: 11109-46.